Available online at www.sciencedirect.com
SCIENCE DIRECT®
Journal of Computational Physics 200 (2004) 432–461
JOURNAL OF COMPUTATIONAL PHYSICS
www.elsevier.com/locate/jcp

Collocation methods for the solution of von-Kármán dynamic non-linear plate systems

Z. Yosibash [a,1], R.M. Kirby [b,*], D. Gottlieb [c]

[a] *Pearlstone Center for Aeronautical Engineering Studies, Department of Mechanical Engineering, Ben-Gurion University, Beer-Sheva, Israel*
[b] *School of Computing, University of Utah, Salt Lake City, UT, USA*
[c] *Division of Applied Mathematics, Brown University, Providence, RI, USA*

Received 8 November 2003; received in revised form 9 March 2004; accepted 10 March 2004
Available online 7 June 2004

Abstract

The von-Kármán nonlinear, dynamic, partial differential system over rectangular domains is considered, and numerically solved using both the Chebyshev-collocation and Legendre-collocation methods for the spatial discretization and the implicit Newmark-β scheme combined with a non-linear fixed point algorithm for the temporal discretization. As the system is non-linear, involving operators of different orders, different timescales, and may contain initial/boundary incompatible conditions at the domain's corners, it is our aim to highlight some of the difficulties inherent in its numerical treatment using collocation methods. We begin by examining the Chebyshev-collocation scheme considered in [Comput. Meth. Appl. Mech. Engrg. 193 (6–8) (2004) 575]. In that work, filtering was used to stabilize the full von-Kármán system, however the source of the instability was not discussed. We first show that IC/BC incompatibilities are not the culprits and demonstrate empirically that the source of the instability was the numerical treatment of the *linear* cross-derivative terms found in the in-plane equations. We prove mathematically that although the continuous linear system is well-posed, the Chebyshev-collocation solution of problems involving cross-derivatives and second-order time derivatives is unstable. Instead of adding sufficient filtering to counter the energy growth due to the linear terms, we employ the Legendre-collocation method. We show empirically and prove that the Legendre-collocation scheme for the linear system has the necessary characteristics to remain stable. Nevertheless, the collocation treatment of the non-linear terms still causes the solution to be unstable at long time. We thus return to advocating a filtering solution, but in this case only filtering the *non-linear* terms to compensate for the inherent aliasing error due to our collocation treatment of these terms. We conclude by comparing the results of filtered Chebyshev-collocation solution, non-linear terms filtered Legendre-

* Corresponding author.
E-mail addresses: zohary@bgu.ac.il (Z. Yosibash), kirby@cs.utah.edu (R.M. Kirby), dig@cfm.brown.edu (D. Gottlieb).
[1] Research performed while the author was on a Sabbatical leave at the Division of Applied Mathematics, Brown University, Providence, RI, USA.

0021-9991/$ - see front matter
doi:10.1016/j.jcp.2004.03.018

collocation solution, and a simplified von-Kármán (solution omitting the inertial terms in the in-plane equations) as presented in (loc. cit).

Keywords: von-Kármán plate model; Chebyshev-collocation; Legendre-collocation; Aliasing; Polynomial filtering

1. Introduction

The von-Kármán plate model is aimed at approximating the elasticity system over a three-dimensional plate-like domain, having one dimension much smaller as compared to the other two. It involves three partial differential equations for the three mid-surface displacements and is time-dependent. Furthermore, as the transverse deformation (deflection) in thin plates may be of the same order of magnitude as the plate thickness, the problem is formulated so to account for large strains/deflections producing non-linear terms.

Due to its complexity, in practical structural engineering applications only very simplified applications of the von-Kármán system are used: for example, the steady-state response for a time-independent model is considered in *static analyses* or *characteristic eigen-frequencies* are sought.

From the mathematical viewpoint, the full von-Kármán system has been shown to be well-posed, admitting a unique solution (bounded for all times) (see, e.g. [2,3]). Most previous numerical investigations addressed either the time *independent* system (see, e.g. [4] and the references therein), or the eigen-frequencies (see, e.g. [5]). In many practical engineering problems, such as the fluid–structure interaction problem of a plate embedded in a flow-field, time-dependent von-Kármán solutions are required, thus the fully non-linear time-dependent von-Kármán system is of interest. This system has been investigated by Nath and Kumar [6] (using Chebyshev series), as well as by Gordnier et al. [7,8] (using finite differences and C^1 h-version finite element methods). In these works, as in [9], it is assumed a priori that terms involving in-plane time derivatives are negligible and are therefore neglected. The neglected terms are the only ones multiplied by the plate thickness, thus neglecting these implies that the solution is thickness independent. Because the system is non-linear and there is no study which quantifies the influence of the in-plane time derivatives on the solution, we herein retain these terms and quantify their influence. Hard-clamped boundary conditions are considered, although other boundary conditions can be easily treated.

The von-Kármán non-linear, dynamic, partial differential system over rectangular domains was formulated and solved by the Chebyshev-collocation method in space and the implicit Newmark-β marching scheme in time (a non-linear fixed point iteration algorithm was employed) in [1] (the detailed numerical analysis and the difficulties associated with the solution process were not addressed). In addition, spatial and temporal numerical errors were addressed as well as some of the idealization errors. We have shown that by considering the "simplified von-Kármán" system, i.e., neglecting four time-dependent terms which are on the order of the square of the plate thickness, one obtains a good approximation of the full von-Kármán solution. At the same time, the simplified system is much more easily tackled by numerical methods as compared to the full system.

However, in view of the instability reported in [1] and the use of a simplified filtering to overcome it, and the mathematical complexity of the full von-Kármán plate model (namely, being a set of three coupled non-linear PDEs involving different orders of spatial derivatives, a bi-harmonic operator for one displacement field and second-order derivatives in the other two displacement fields including mixed derivatives, first- and second-order time derivatives, different timescales between the three displacement fields), special attention is required when numerical approximations are sought. We demonstrate herein that our initial hypothesis that incompatibilities between the initial and boundary conditions as described in [10] were not to blame for the instabilities. Rather, we tracked the problem down to the Chebyshev-collocation treatment of the linear cross-derivative terms. We show that Chebyshev-collocation methods applied to cross-derivative terms in second-order time problems is unstable. The instability of the linear terms may be relieved

by using a Legendre-collocation scheme. Although we can both empirically show and prove mathematically that the Legendre-collocation solution of the linear problem is stable, the non-linear system does not remain stable for long-time. The von-Kármán system of interest is non-linear and thus non-linear aliasing due to our collocation treatment of the non-linear terms is a further culprit in the stability of our scheme. We show how filtering of the non-linear terms only is one means of solving this problem.

Specifically, we present herein the following:

- The non-dimensional form of the full von-Kármán system for an isotropic plate and the different sources of difficulties associated with its numerical approximation.
- We then proceed to provide a short outline of the numerical algorithms used for the spatial and temporal discretizations. For spatial approximations, we use a collocation method. We will briefly discuss both Chebyshev and Legendre methods of this form. For time discretization, we used a second-order implicit Newmark-β time marching scheme in conjunction with a fixed point iteration technique *without linearization*. We provide discussion of the simple filtering algorithm used in our previous work [1], and discuss an alternative filtering technique which we will use in the Legendre-collocation case presented herein.
- We present numerical results demonstrating that the Chebyshev-collocation scheme for the full von-Kármán system is unstable. In [1], we hypothesized that initial condition and boundary condition incompatibility may have been the culprit. We demonstrate that this is not the case. Even with specially crafted initial conditions, boundary conditions and forcing functions we still arrived at an unstable scheme. We then empirically deduced that the problem lie with the *linear* cross-derivative terms in the hyperbolic equations for u and v (the in-plane displacements). We provide numerical results to demonstrate that by dropping the cross-derivative terms $u_{,12}$ and $v_{,12}$ one eliminates the instability, however, at a cost of a modeling error which is visible in the solution of w (the plate deflection in the normal direction). By solving a very simple linear problem, we demonstrate that the numerical discretization of the linear terms (in particular the cross-derivative terms) is unstable.
- We then attempt to isolate the true source of the instability. We first verify that the Chebyshev-collocation method applied to the linear terms is consistent (which it is). We then, by Kreiss analysis, prove that the mathematical continuous system is well-posed. We then show through discrete eigenanalysis that the source of the instability comes from the eigenvalue distribution induced by the Chebyshev-collocation method applied to the linear terms in the full von-Kármán system.
- The instability because of the mixed spatial derivatives can be overcome by using the Legendre-collocation method. We demonstrate that it is stable for the linear system, however suffers from long time instabilities due to aliasing generated by our collocation treatment of the non-linear terms in the in-plane hyperbolic equations. To overcome the long-time instability, we apply exponential filtering (removing the high-frequency growing terms) for the non-linear part in the in-plane equations, and provide numerical results showing the regain of the stability. We compare these results with the ones reported in [1] where the Chebyshev-collocation methods with "average filtering" used for u and v solutions (which is equivalent to adding structural dissipation), for which the time instabilities disappear.
- We also consider the "simplifiedvon-Kármán system", i.e., neglecting the time derivative terms in the in-plane equations (which are of order of the plate thickness squared in comparison with the order one other terms). This simplified system provides transverse displacements (w) which are in very good agreement with the ones obtained by solving the full system. At the same time, the simplified system does not suffer from instability problems, as will be explained.

The von-Kármán system, notations, and non-dimensionalization are presented in Section 2. In this section, we discuss also the spatial discretization by means of the Chebyshev-collocation and Legendre-collocation methods in conjunction with a temporal discretization using the Newmark-β scheme. Two filtering algorithms are also briefly outlined. We provide in Section 3 numerical experiments demonstrating the performance of the Chebyshev-collocation method for the von-Kármán system showing the instabilities in time. We discuss the sources of instability in Section 4 where an analysis of the continuum linear system

is provided, followed by a mathematical analysis of the discretized problem, explaining the reason for the instability. We then proceed to present in Section 5 the numerical results obtained by the Legendre-collocation method, demonstrating that we regain stability in the linear range, and show its performance when exponential filtering is applied to the non-linear terms in the in-plane equations. We also compare the results to those obtained by the Chebyshev-collocation method with filtering, and with these obtained for the simplified system. A summary, conclusions and open topics of future research are provided in Section 6.

2. Notations, problem formulation, and numerical scheme

Following [4,9,11] we derived in [1] the equations describing the von-Kármán plate model made of an isotropic elastic material, and we present herein the final outcome which are the three equations of interest in non-dimensional form. We then present a discussion of the spatial and numerical discretization of the von-Kármán system employing the Chebyshev- and Legendre-collocation method in space and Newmark-β scheme in time. We also present a brief discussion of the filtering techniques used.

2.1. Notations and problem formulation

Consider a square plate of dimensions $a \times a \times h^*$ (quantities denoted by asterisk, *, are dimensional quantities which have a non-dimensionalized counterpart) with the assumption that $h^* \ll a$. The Cartesian coordinate system is denoted by $\mathbf{x}^* = (x_1^* \; x_2^* \; x_3^*)^{\mathrm{T}}$, where the plate thickness is in the x_3^*-direction, and $\mathbf{u}^*(x_1^*, x_2^*, t^*) = (u^* \; v^* \; w^*)^{\mathrm{T}}$ is the mid-plane displacement vector in the corresponding directions (see Fig. 1).

Let E^*, ν, c^*, ρ^* denote the Young modulus, Poisson ratio, structural viscosity coefficient and density of the plate's material. We assume no body forces are applied on the plate, and on its upper and lower surfaces, traction loading in the x_3^*-direction $g_3^{*\pm\frac{h^*}{2}}$ is applied. These are of course prescribed functions of x_1^*, x_2^* and t^* alone.

Following [6], we perform the following change of variables:

$$u = \frac{(a/2)u^*}{(h^*)^2}, \quad v = \frac{(a/2)v^*}{(h^*)^2}, \quad w = \frac{w^*}{(h^*)}, \quad x_1 = \frac{x_1^*}{(a/2)}, \quad x_2 = \frac{x_2^*}{(a/2)},$$

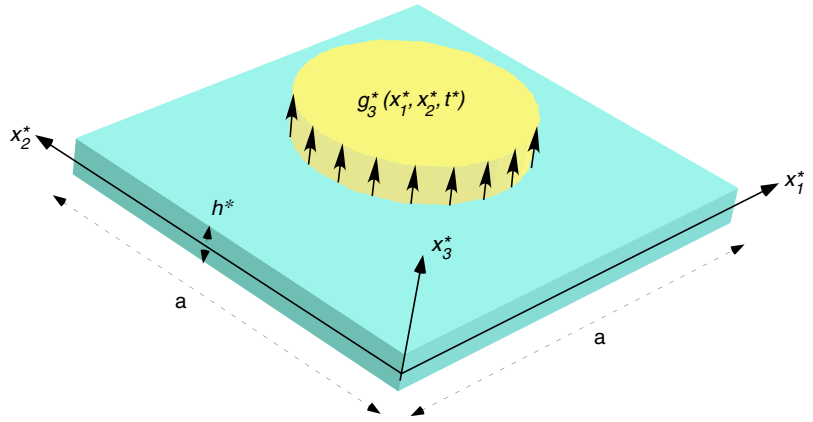

Fig. 1. Notations for plate of interest.

$$t = t^*\sqrt{\frac{D^*}{\rho^* h^* (a/2)^4}} \quad g = \frac{g^*(a/2)^4}{D^* h^*}, \quad h = \frac{h^*}{(a/2)}, \quad c = c^*\sqrt{\frac{(a/2)^4 h^*}{\rho^* D^*}},$$

where $D^* \stackrel{\text{def}}{=} E^*(h^*)^3/(12(1-\nu^2))$ is the flexural rigidity.

With the above set of non-dimensional variables, the full non-dimensional von-Kármán system over a quadrilateral domain $\Omega = [0,2] \times [0,2]$ is given by the following three coupled equations:

$$w_{,tt} + cw_{,t} + \nabla^4 w - 12\Big[(u_{,1} + \tfrac{1}{2}w_{,1}^2)(w_{,11} + \nu w_{,22}) + (v_{,2} + \tfrac{1}{2}w_{,2}^2)(w_{,22} + \nu w_{,11}) + (1-\nu)(v_{,1} + u_{,2} + w_{,1}w_{,2})w_{,12}\Big] = g_3, \tag{1}$$

$$\frac{h^2}{6}(u_{,tt} + cu_{,t}) - [2u_{,11} + (1+\nu)v_{,12} + (1-\nu)u_{,22} + 2w_{,1}w_{,11} + (1+\nu)w_{,2}w_{,12} + (1-\nu)w_{,1}w_{,22}] = 0, \tag{2}$$

$$\frac{h^2}{6}(v_{,tt} + cv_{,t}) - [2v_{,22} + (1+\nu)u_{,12} + (1-\nu)v_{,11} + 2w_{,2}w_{,22} + (1+\nu)w_{,1}w_{,12} + (1-\nu)w_{,2}w_{,11}] = 0. \tag{3}$$

The system is accompanied by Dirichlet boundary conditions (denoted by "hard clamped") which are:

$$u = v = w = \partial_n w = 0 \quad \text{on } \partial\Omega. \tag{4}$$

Remark 1. The first two time-dependent terms in (2) and (3) are of order h^2 compared to the order one terms in the rest of the equations, and so are commonly neglected (see [4,6,8] for example). This set of equations will be denoted as the *simplified von-Kármán* system, as opposed to the *full von-Kármán* system (1)–(3). The simplified von-Kármán system considerably simplifies its numerical treatment as one is left with one prognostic Eq. (1) with two "constraint equations", a set which is much easier to solve. Nath and Kumar [6] and Gordnier and Visbal [8] considered the simplified von-Kármán system of equations.

Remark 2. In the complete von-Kármán set of equations, another term, $-(h^2/12)\Delta w_{,tt}$, appears in (1) as a consequence of rotational inertia. This term, although technically necessary for the mathematical proof that the von-Kármán system has a unique solution (see [2,3]), has no influence on the numerical treatment of the equations, and is neglected in all engineering applications. Therefore, it has not been considered in our formulation. Numerical experiments *with* the rotational inertial term demonstrate that it does not change the characteristics of our numerical method.

2.2. The numerical scheme

We solve numerically the von-Kármán plate model using collocation methods (both Chebyshev and Legendre) [12,13] for the spatial discretization and the Newmark-β scheme [14] for integration in time. We now briefly discuss both of these components.

2.2.1. Spatial discretization

Collocation methods [12,13] as well as high-order finite element methods [15,16] were shown to be efficient for spatial-discretization, yielding in "exponential (spectral) converge rates", and have been used in [6,5] for the solution of variants of the von-Kármán system. Collocation method can easily treat the nonlinear terms and are a natural choice for quadrilateral domains, and thus has been adopted in the present work (differences compared to [6] with respect to the handling of the boundary conditions and the nonlinear terms are detailed in [1]).

As a brief review, the fundamental concept of collocation methods is to seek polynomial approximations which "collocate" the differential operators, that is, which satisfy the differential equation at a finite number of points. Collocation methods can be viewed as members of the weighted residual methods with the test functions being chosen as delta functions at a finite number of carefully prescribed points [16].

What differentiates different collocation methods is the choice of points used to collocate the differential operator. Chebyshev-collocation methods collocate at the Chebyshev–Gauss–Lobatto points, whereas Lengendre-collocation methods collocate at the Legendre–Gauss–Lobatto points. Although once the point distribution has been decided the development of the collocations schemes follows a prescribed pattern, the properties of the scheme is highly dependent on which point distribution is used [12,13].

We will now briefly outline the way in which collocation methods were used in this work. For simplicity of discussion, we will use the term point distribution to refer to either the Chebyshev or Legendre point distribution. Suppose that we are provided a point distribution of $N+1$ points on $[-1,1]$. We begin by discretizing the interval $[0,2]\times[0,2]$ using a mapping of the tensor product of the point distribution. We denote the tensor product point distribution on $[0,2]\times[0,2]$ by $((x_1)_j,(x_2)_k)$ where $j,k=0,\ldots,N$ (for simplicity $(x_1)_i>(x_1)_j\ \forall i>j$ and similarly for x_2). Given a function $u(x_1,x_2)$, we can define its Nth order polynomial interpolant:

$$u_N(x_1,x_2)=\mathscr{I}_N u(x_1,x_2)=\sum_{i=0}^{N}\sum_{j=0}^{N}u((x_1)_i,(x_2)_j)h_i(x_1)h_j(x_2), \tag{5}$$

where $h_i((x_1)_k)=\delta_{ik}$ denotes the ith Lagrange interpolating polynomial based upon the point set $\{(x_1)_k\}$. The function $h_j((x_2)_k)$ is similarly defined. The fundamental premise of collocation methods is that given $u_N(x_1,x_2)$ we can then form approximations of the derivatives of u as:

$$\frac{\mathrm{d}^n u(x_1,x_2)}{\mathrm{d}x_1^n}\approx\frac{\mathrm{d}^n u_N(x_1,x_2)}{\mathrm{d}x_1^n}=\frac{\mathrm{d}^n}{\mathrm{d}x_1^n}\mathscr{I}_N u(x_1,x_2)=\sum_{i=0}^{N}\sum_{j=0}^{N}u((x_1)_i,(x_2)_j)\frac{\mathrm{d}^n h_i(x_1)}{\mathrm{d}x_1^n}h_j(x_2).$$

A similar statement can be made for derivatives in the x_2-direction. Two important algorithmic points stem from this formulation: (1) derivatives of one-dimensional interpolants are formulated as a matrix–vector multiplication of a derivative matrix operator times a vector of grid values and (2) derivatives in one direction of a two-dimensional interpolant can be implemented as the successive application of the one-dimensional derivative operator. For detailed discussions of both the mathematical and implementation details of collocation methods, we refer the reader to [12,13].

The homogeneous Dirichlet boundary conditions are incorporated strongly by adjusting the discrete differential operators. For first- and second-order spatial operators, strong treatment is very common and widely discussed [12,13]. Special attention, however, is required for the function w as its normal derivative in addition to its value are zero at the boundaries. To enforce both boundary conditions for w in the strong form simultaneously, we represent w as polynomial of the form:

$$w(x_1,x_2)=(1-x_1^2)(1-x_2^2)q(x_1,x_2). \tag{6}$$

This particular choice automatically satisfies the boundary conditions $w(\pm1,x_2)=w(x_1,\pm1)=0$ and if in addition one requires that $q(\pm1,x_2)=q(x_1,\pm1)=0$ then also the normal derivatives of w are identically zero on the boundary. Substituting (6) into a bi-harmonic operator, for example, one obtains the following bi-harmonic operator in terms of $q(x_1,x_2)$:

$$\begin{aligned}&(1-x_2^2)\Big((1-x_1^2)\partial_{x_1}^4-8x_1\partial_{x_1}^3-12\partial_{x_1}^2\Big)q(x_1,x_2)+(1-x_1^2)\Big((1-x_2^2)\partial_{x_2}^4-8x_2\partial_{x_2}^3-12\partial_{x_2}^2\Big)q(x_1,x_2)\\&\quad+2\Big(4+8x_2\partial_{x_2}^2+8x_1\partial_{x_2}-2(1-x_1^2)\partial_{x_1}^2-2(1-x_2^2)\partial_{x_2}^2+16x_1x_2\partial_{x_1}\partial_{x_2}-4x_1(1-x_2^2)\partial_{x_1}\partial_{x_2}^2\\&\quad-4x_2(1-x_1^2)\partial_{x_1}^2\partial_{x_2}+(1-x_1^2)(1-x_2^2)\partial_{x_1}^2\partial_{x_2}^2\Big)q(x_1,x_2)=\nabla^4 w(x_1,x_2).\end{aligned} \tag{7}$$

All other differential operators on w are treated similarly, resulting in a system involving the unknown functions u, v, q which are restricted to be zero on the boundaries. A discussion of implementing boundary conditions of this form is presented in [1].

Using the methodology as discussed above, the von-Kármán system (1)–(3) is solved in a *point-wise* fashion where spatial derivative operators are replaced by the appropriate discrete collocation derivative operators. This form of discretization allows for easy implementation of the non-linear terms; non-linearities are handled by point-wise evaluation at the collocation points.

2.2.2. Temporal discretization

To discretize the von-Kármán system in time, we have chosen to employ the the average acceleration variant of the Newmark-β scheme [14] (with Newmark parameters $\gamma = \frac{1}{2}$ and $\beta = \frac{1}{4}$) which exhibits second-order convergence in time and is unconditionally stable under linear analysis.

The variant of the Newmark-β scheme which we employed can be algorithmically described as follows. Assume one is given the equation:

$$m\ddot{u} + c\dot{u} + ku = g, \tag{8}$$

where the forcing g may be a function of the solution u. Discretizing in time we obtain the expressions at time level n and $n+1$, respectively:

$$\begin{aligned} &m\ddot{u}_n + c\dot{u}_n + ku_n = g_n, \\ &m\ddot{u}_{n+1} + c\dot{u}_{n+1} + ku_{n+1} = g_{n+1}. \end{aligned} \tag{9}$$

The average acceleration variant of the Newmark-β scheme (see [14]) is given by the following time difference equations:

$$\begin{aligned} \dot{u}_{n+1} &= \dot{u}_n + \frac{\Delta t}{2}\left(\ddot{u}_n + \ddot{u}_{n+1}\right), \\ u_{n+1} &= u_n + \Delta t\dot{u}_n + \frac{(\Delta t)^2}{4}\left(\ddot{u}_n + \ddot{u}_{n+1}\right), \end{aligned} \tag{10}$$

where the local truncation error of these equations is $\mathcal{O}(\Delta t^2)$. We can now combine Eqs. (9) and (10) to yield the following equation for the solution u at time level $n+1$ given information at time level n and the forcing function g at time level $n+1$:

$$\left(\frac{4m}{(\Delta t)^2} + \frac{2c}{\Delta t} + k\right)u_{n+1} = g_{n+1} + m\left(\frac{4}{(\Delta t)^2}u_n + \frac{4}{\Delta t}\dot{u}_n + \ddot{u}_n\right) + c\left(\frac{2}{\Delta t}u_n + \dot{u}_n\right). \tag{11}$$

The von-Kármán system however, is not linear, and hence we employ the fixed point method of solving a non-linear system of equations [17]. This can be understood as follows. First, define the solution vector as $\vec{u} = (\hat{u}(x_1, x_2, t), \hat{v}(x_1, x_2, t), \hat{w}(x_1, x_2, t))^{\mathrm{T}}$. We can thus re-write (1)–(3) as:

$$\frac{\partial^2 \vec{u}}{\partial \hat{t}^2} + \hat{c}\frac{\partial \vec{u}}{\partial \hat{t}} = G(\vec{u}),$$

where we have grouped all the linear, non-linear and forcing terms into the expression $G(\vec{u})$. We now discretize this system in time using Eq. (11) to obtain:

$$\left(\frac{4}{(\Delta t)^2} + \frac{2\hat{c}}{\Delta t}\right)\vec{u}_{n+1} = G(\vec{u}_{n+1}) + \left(\frac{4}{(\Delta t)^2}\vec{u}_n + \frac{4}{\Delta t}\dot{\vec{u}}_n + \ddot{\vec{u}}_n\right) + \hat{c}\left(\frac{2}{\Delta t}\vec{u}_n + \dot{\vec{u}}_n\right).$$

The equation above can easily be re-cast in the following form:

$$\vec{u}_{n+1} = \tilde{G}(\vec{u}_{n+1}), \tag{12}$$

where we have grouped all the terms involving information at time level n and all non-linear and forcing terms into the expression $\tilde{G}$. Written in this form, we see that this is a candidate for the fixed point method. Henceforth, for all our von-Kármán tests, we employ this combination of the Newmark-β scheme with the fixed point iteration method.

Remark 3. The fixed point iteration requires an initial guess to initiate the iteration. We have chosen the solution at the previous time step n for solving for the solution at the time step $n+1$. Other initial guesses have been also tested (taking $u = v = 0$ for example) and shown to provide same solution at time step $n+1$.

Remark 4. For the full von-Kármán system, the time step restriction imposed by the fixed point iteration seemed to be linearly proportional to the plate thickness. The thinner the plate, the smaller the time step was required for the Lipschitz constant to be less than one (a condition which is necessary to guarantee that the fixed point method will converge).

Remark 5. The discussion above for the full von-Kármán system can be modified to encompass the simplified von-Kármán system. A complete discussion of the necessary modification is presented in [1].

2.3. Filtering

One of the methods to overcome instabilities associated with growing solutions, aliasing errors, etc., is the method of filtering [12]. Algorithmically, one may view filtering as follows. Given a polynomial function $u_N(x_1, x_2)$ as in (5), one can also uniquely write the polynomial in the following form [12]:

$$u_N(x_1, x_2) = \sum_{i=0}^{N} \sum_{j=0}^{N} \hat{u}_{ij} L_i(x_1) L_j(x_2), \tag{13}$$

where $L_i(x_1)$, for example, denotes the ith Legendre polynomials, respectively. Based upon the properties of the Legendre polynomials [12], we have that:

$$\hat{u}_{ij} = \frac{1}{\gamma_i} \frac{1}{\gamma_j} \langle u(x_1, x_2), L_i(x_1) L_j(x_2) \rangle, \tag{14}$$

where $\langle \cdot, \cdot \rangle$ denotes the L^2 inner product and $\gamma_n = 2/(2n+1)$.

The idea of filtering is to modify the modal coefficients $\hat{u}_{ij}$ in some well-described manner, normally in a way in which the "high (spatial) frequencies" (i.e., high modal numbers) are attenuated. This attenuation process can be viewed as selectively adding dissipation to the numerical scheme (but only at the high modes of the function; hence many people view this process as merely adding a low-pass filter operator). We define a filter $\sigma(\eta) : [0,1] \to [0,1]$ where η at discrete values η_n is given by:

$$\eta_n = \frac{\lambda_n}{\lambda_N} = \frac{n(n+1)}{N(N+1)},$$

with λ_n denoting the nth eigenvalue of the Sturm–Liouville problem for the Legendre polynomials. The operation of filtering a function $u_N(x_1, x_2)$ is defined as follows:

$$\mathscr{F} u_N(x_1, x_2) = \sum_{i=0}^{N} \sum_{j=0}^{N} \Big(\sigma(\eta_i) \sigma(\eta_j) \hat{u}_{ij} \Big) L_i(x_1) L_j(x_2). \tag{15}$$

In [1], we used for the Chebyshev-collocation method a simple discrete filtering scheme $\tilde{\mathscr{F}}$ at every M steps (where M was determined empirically). The simple filtering operator $\tilde{\mathscr{F}}$ is defined by

$$\tilde{\mathscr{F}}(u(x_i,x_j)) = \tfrac{1}{8}\big(u(x_{i+1},x_j) + u(x_{i-1},x_j) + 4u(x_i,x_j) + u(x_i,x_{j+1}) + u(x_i,x_{j-1})\big),$$

where $i,j = 1,\ldots,N-1$. This filter is the discrete analog of the second-order raised-cosine filter [12] given by:

$$\sigma_{\mathrm{C}}(\eta) = 0.5(1+\cos(\pi\eta))$$

in the filtering discussion presented above. In Fig. 2, we present a plot of $\sigma_{\mathrm{C}}(\eta)$ demonstrating how all spatial frequencies are effected by the filter, however the most pronounced attenuation occurs at the highest frequencies.

Both in [1] and throughout this paper, when we refer to filtering in the context of the Chebyshev-collocation implementation of the von-Kármán system we are referring to the discrete filter $\tilde{\mathscr{F}}$ applied *only* to the u and v (in-plane) solutions.

A better filtering method uses the exponential filter function $\sigma_{\mathrm{E}}(\eta_n)$ (see [12]):

$$\sigma_{\mathrm{E}}(\eta_n) = \exp(-\alpha\eta_n^p), \tag{16}$$

where p denotes the order of the filter and where α is a scaling parameter (normally taken to be $\alpha = -\log(\epsilon_{\mathrm{M}})$, where $\epsilon_{\mathrm{M}} = 10^{-14}$ is the standard machine zero). In Fig. 3, we plot $\sigma_{\mathrm{E}}(\eta)$ for varying orders p.

Herein, when applying the Legendre-collocation method to the full von-Kármán system, we will need to filter the non-linear terms in the in-plane Eqs. (2) and (3) so as to regain stability (we will discuss this point more fully in Section 5). These non-linear terms of the in-plane equations are given by:

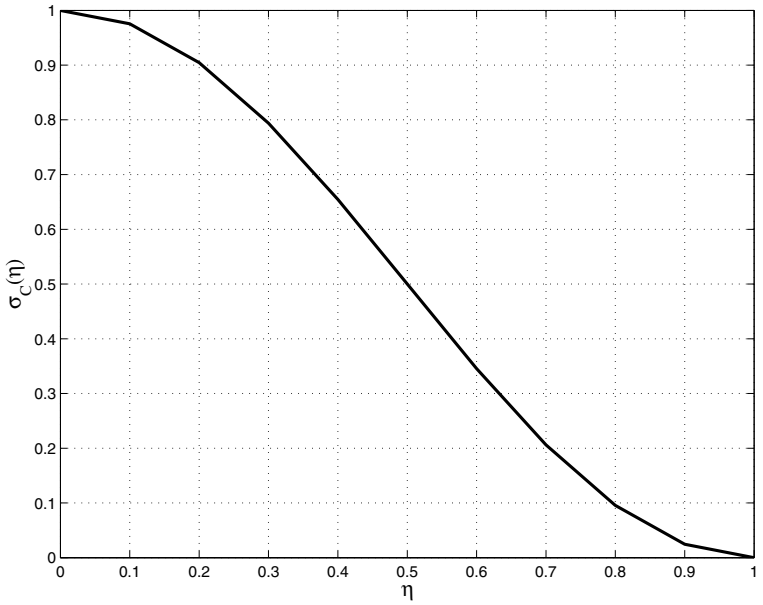

Fig. 2. The filter function $\sigma_{\mathrm{C}}(\eta)$.

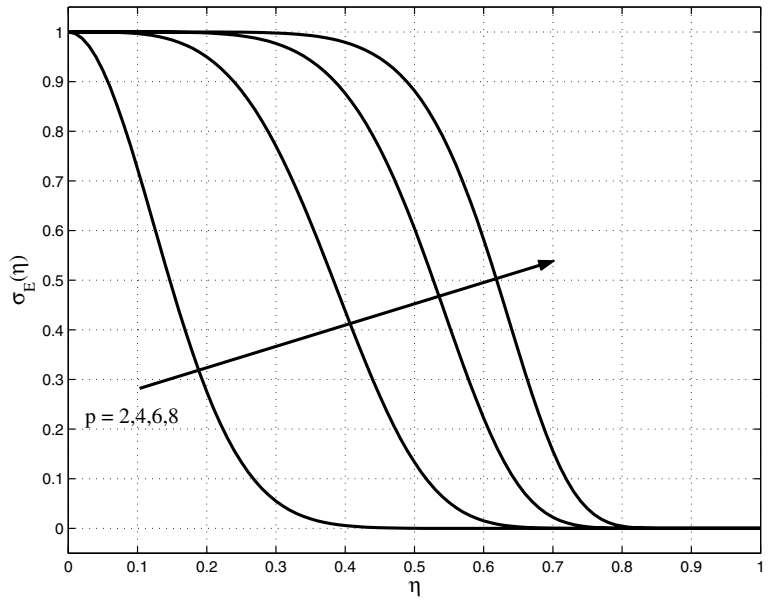

Fig. 3. The filter function $\sigma_E(\eta)$ for increasing values of p.

$$\mathrm{NLT}_u(x_1,x_2) = 2w_{,1}w_{,11} + (1+\nu)w_{,2}w_{,12} + (1-\nu)w_{,1}w_{,22}, \tag{17}$$

$$\mathrm{NLT}_v(x_1,x_2) = 2w_{,2}w_{,22} + (1+\nu)w_{,1}w_{,12} + (1-\nu)w_{,2}w_{,11}. \tag{18}$$

In the solution of the in-plane equations, we accomplish the following:

- We compute all relevant derivative quantities (i.e., $w_{,1}, w_{,2}$, etc.) using collocation derivative matrices.
- We compute the non-linear terms on the collocation grid.
- Using Gaussian quadrature to approximate integration, we find the modal coefficients of the Legendre expansion (Eq. (13)) as given by Eq. (14).
- Using the exponential filter as defined in Eq. (16), we filter the polynomial expansion coefficients as done in Eq. (15).
- We evaluate the filtered polynomial expansion at the grid points to yield the filtered non-linear terms on the collocation grid.

We then combine additively the result of the above procedure with the linear terms of the in-plane equations and integrate in time. Note that unlike the Chebyshev case, we do not filter the solution u and v, but merely the evaluation of the non-linear terms in the u and v equations. This will play an important point in Section 5.

3. Chebyshev-collocation: spatial convergence, and temporal instability

The numerical formulation in the previous section, employing the Chebyshev-collocation method is used for solving the full von-Kármán (1)–(3) having clamped boundaries according to Eq. (4). For convenience, we chose to use $\nu = 0.3$ in our numerical experiments.

3.1. Instabilities in the full system for the Chebyshev-collocation method

Consider a constant load $g = 29.6$ applied on the plate having a thickness $h = 0.1$ and $c = 1.25$. We use a $N \times N$ collocation grid with $N = 9, 11, 13, 15$ and $\Delta t = 10^{-6}$ and report the midpoint deflection $w(1,1,t)$ in Fig. 4.

Using now $N = 13$ collocation grid and varying $\Delta t = 10^{-6}, 10^{-7}, 10^{-8}$, we report the midpoint deflection $w(1,1,t)$ in Fig. 5.

As noticed, an instability develops which causes the divergence of the solution at a very short time, independent of the time step Δt. Also, the total time until instability develops appears to be inversely proportional to the interpolation order N of the collocation method.

Our first hypothesis as to the source of the instability (as discussed in [1]) was an incompatibility between the initial and boundary conditions was inducing an instability. In Section 3.2, we will dispel this idea and show empirically that the instability still exists even when no incompatibility exists. In Section 3.3, we will then outline through numerical examples on the source of the instability.

3.2. Incompatible initial-boundary conditions at the corner

It is known that singularities may arise due to incompatible boundary and initial conditions associated with a PDE (see survey in [10]). In the von-Kármán system with hard-clamped boundary conditions and zero initial conditions (velocities are zero), and a constant applied load $g = \text{const.}$, incompatible IC/BC may occur at the vertices. To illustrate this point, let us consider the vertex $(0,0)$ for example. Due to the boundary condition $u = v = w = 0$ along the x_1-axis, then at the vertex $(0,0)$ u, v, w have zero ∂_2^n derivatives for any $n = 0, 1, 2, 3, \ldots$ A similar argument holds for the x_2-axis, so that at the vertex $(0,0)$ u, v, w have zero ∂_1^n derivatives for any $n = 0, 1, 2, 3, \ldots$ Thus at $x_1 = x_2 = 0$ and $t = 0$, the system (1)–(3) becomes:

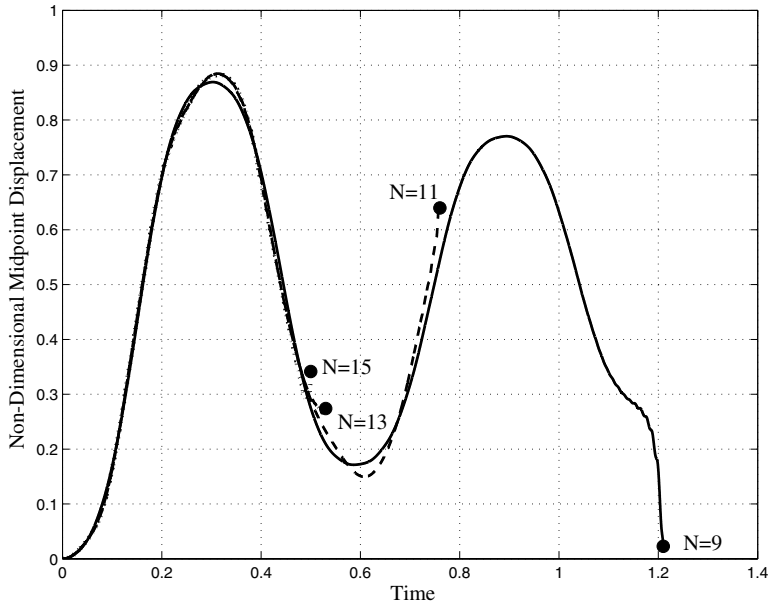

Fig. 4. Chebyshev-collocation: Midpoint displacement $w(1,1,t)$ for varying spatial resolution N. Solid line $N = 9$, dashed $N = 11$, dash-dot $N = 13$ and dotted $N = 15$. The circles denote the approximate time at which solution becomes unstable. $\Delta t = 10^{-6}$, $h = 0.1$, $c = 1.25$, $g = 29.60$, Fixed point conv. tolerance 10^{-10}. No filtering was used.

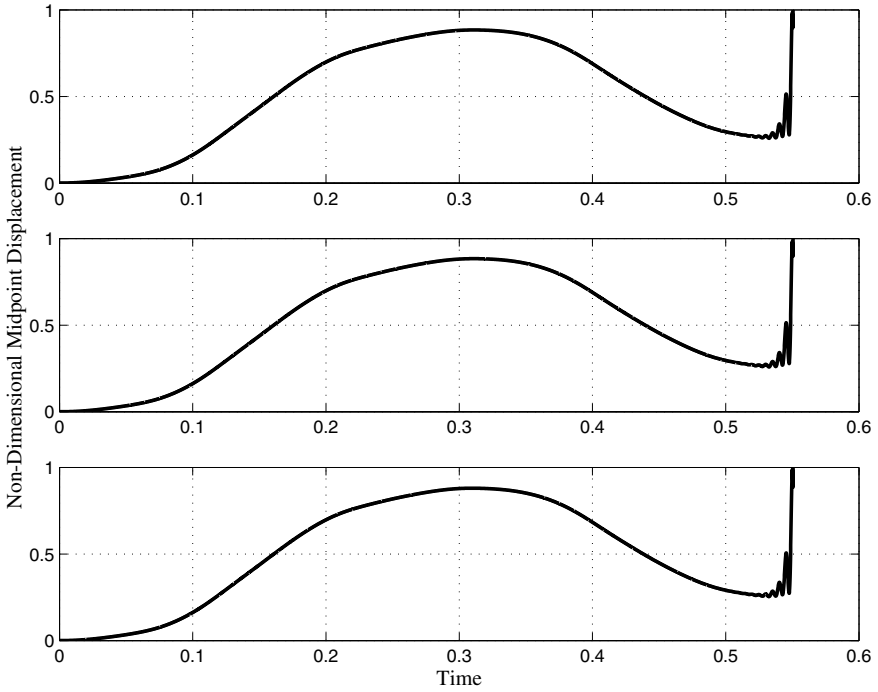

Fig. 5. Chebyshev-collocation: Midpoint displacement $w(1,1,t)$ for varying Δt. Top, $\Delta t = 10^{-6}$, middle $\Delta t = 10^{-7}$, bottom $\Delta t = 10^{-8}$. $N = 13$, $h = 0.1$, $c = 1.25$, $g = 29.60$, Fixed point conv. tolerance 10^{-10}. No filtering was used.

$$w_{,tt}(0,0,0) + cw_{,t}(0,0,0) = g_3(0,0,0), \tag{19}$$

$$\frac{(2\varepsilon)^2}{6}\left(u_{,tt}(0,0,0) + cu_{,t}(0,0,0)\right) = 0, \tag{20}$$

$$\frac{(2\varepsilon)^2}{6}\left(v_{,tt}(0,0,0) + cv_{,t}(0,0,0)\right) = 0. \tag{21}$$

Because of the zero velocity initial conditions at $t = 0$, (19)–(21) become:

$$w_{,tt}(0,0,0) = g_3(0,0,0), \tag{22}$$

$$u_{,tt}(0,0,0) = 0, \tag{23}$$

$$v_{,tt}(0,0,0) = 0, \tag{24}$$

so for a Heaviside function $g_3 = \begin{cases} 0 & t < 0 \\ \text{const.} & t \geqslant 0 \end{cases}$, it is an incompatible equation, giving rise to space-time singular behavior.

To investigate, if this phenomenon was the source of our instability, three different loadings are considered:

$$g_3 = 29.6, \tag{25}$$

$$g_3 = 106.4 \sin^2(\pi x_1/2) \sin^2(\pi x_2/2), \tag{26}$$

$$g_3 = 106.4(1 - \mathrm{e}^{-t}) \sin^2(\pi x_1/2) \sin^2(\pi x_2/2), \tag{27}$$

where the leading coefficient has been chosen so that all three forces have same integral value taken over the plate $[0,2] \times [0,2]$ (for (27) this statement is valid for very large t).

The loading in (25), clearly does not satisfy (22), producing space–time singular behavior. Loading (26) and (27) both satisfy (22), however, (26) is a Heaviside function in time: At $t = 0$, because there velocities and accelerations are zero, one has:

$$\begin{aligned}
&\nabla^4 w - 12\Big[(u_{,1} + \tfrac{1}{2}w_{,1}^2)(w_{,11} + \nu w_{,22}) + (v_{,2} + \tfrac{1}{2}w_{,2}^2)(w_{,22} + \nu w_{,11}) + (1-\nu)(v_{,1} + u_{,2} + w_{,1}w_{,2})w_{,12}\Big] \\
&\quad = g_3(x_1, x_2, 0), \\
&-[2u_{,11} + (1+\nu)v_{,12} + (1-\nu)u_{,22} + 2w_{,1}w_{,11} + (1+\nu)w_{,2}w_{,12} + (1-\nu)w_{,1}w_{,22}] = 0, \\
&-[2v_{,22} + (1+\nu)u_{,12} + (1-\nu)v_{,11} + 2w_{,2}w_{,22} + (1+\nu)w_{,1}w_{,12} + (1-\nu)w_{,2}w_{,11}] = 0.
\end{aligned}$$

The loading in (27) eliminates all these problems, and hence in the context of this discussion is a "nice" loading for which we would expect no instabilities due to incompatibilities.

The solutions obtained using (25)–(27) are all unstable. In Fig. 6, we plot the midpoint displacement $w(1,1,t)$ given the three different forcing functions for a fixed N and Δt. All three solutions eventually become unstable. For this empirical test, we deduced that the incompatibility conditions were not to blame for the instability and that the source of the problem is elsewhere.

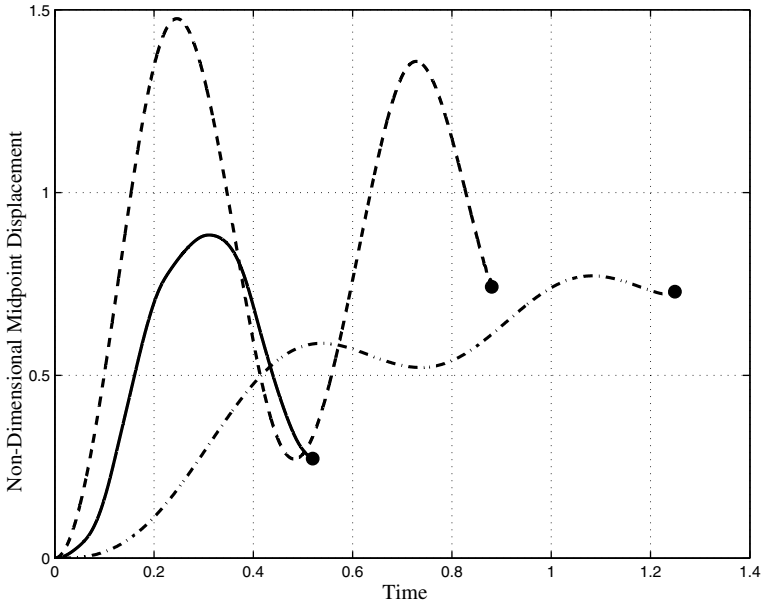

Fig. 6. Chebyshev-collocation: Midpoint displacement $w(1,1,t)$ given three different forcing functions. The solid line was produced using (25); the dashed line was produced using (26); and the dash-dot line was produced using (27). The circles denote the approximate time at which solution becomes unstable. $N = 13$, $\Delta t = 10^{-6}$, $h = 0.1$, $c = 1.25$, Fixed point conv. tolerance 10^{-10}. No filtering was used.

3.3. The source of the instability

Through numerical experimentation, we determined that the source of the instability can be attributed to the Chebyshev-collocation spatial discretization of the *linear* cross-derivative terms in in-plane equations.

To arrive at the hypothesis that the cross-derivative terms were the culprits, we examined contour plots of the in-plane solutions. In Fig. 7, we show the in-plane displacement $u(x_1, x_2, t)$ evolution which better illuminates the instability propagation. Same typical behavior is evident for the in-plane displacement $v(x_1, x_2, t)$.

Upon examination of these plots, we hypothesized that the instability was initiated near the corners of the domain where cross-derivative terms would have a pronounced effect. To test our hypothesis, we ran the full von-Kármán system given by Eqs. (2) and (3) with the cross-derivative terms ($u_{,12}$ and $v_{,12}$) removed (but all other terms being present in the equations). In Fig. 8, we present the full von-Kármán solution with and without the cross-derivative terms.

One observes that the von-Kármán system without the mixed derivative terms is stable, whereas the full system is not. One might naively decide that if the cross-derivative terms are the source of the instability, then omitting them is a viable option. Comparison with known solutions for the particular case shown above yield that the modeling error due to this assumption can be as high at 5% (examined over the interval $t \in [0.2, 0.5]$).

To further establish if examining the linear system was sufficient for understanding the source of the instability, we solved the following simplified model of the in-plane equations:

$$\frac{h^2}{6}(u_{,tt} + cu_{,t}) = 2u_{,11} + (1+v)v_{,12} + (1-v)u_{,22} + f_1, \tag{28}$$

$$\frac{h^2}{6}(v_{,tt} + cv_{,t}) = (1-v)v_{,11} + (1+v)u_{,12} + 2v_{,22} + f_2, \tag{29}$$

with u and v being zero on the boundaries and initial conditions of zero displacement and zero velocity at time $t = 0$. In Fig. 9, we plot the midpoint displacement of u when applying a constant force $f_1 = f_2 = 1.0$ ($N = 13$, $\Delta t = 10^{-5}$, $h = 0.1$, $c = 1.25$, Fixed point conv. tolerance 10^{-10}). Even this very simple linear example, when solved using a Chebyshev-collocation method, exhibits an instability, and hence this very simple linear system will be scrutinized to determine the source of the instability.

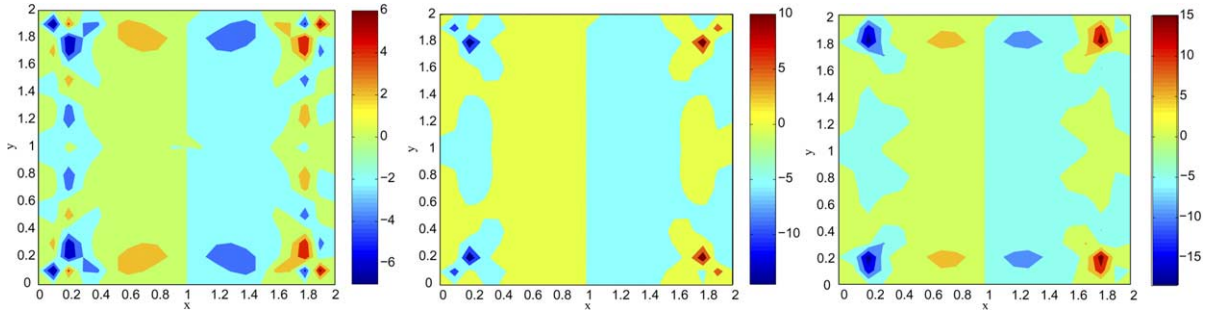

Fig. 7. Chebyshev-collocation: Flood contour plot of the in-plane displacement $u(x_1, x_2, t)$ at $t = 0.548$ (left), $t = 0.549$ (center), and $t = 0.550$ (right). $\Delta t = 10^{-6}$, $N = 13$, $h = 0.1$, $c = 1.25$, $g = 29.60$, Fixed point conv. tolerance 10^{-10}. No filtering was used.

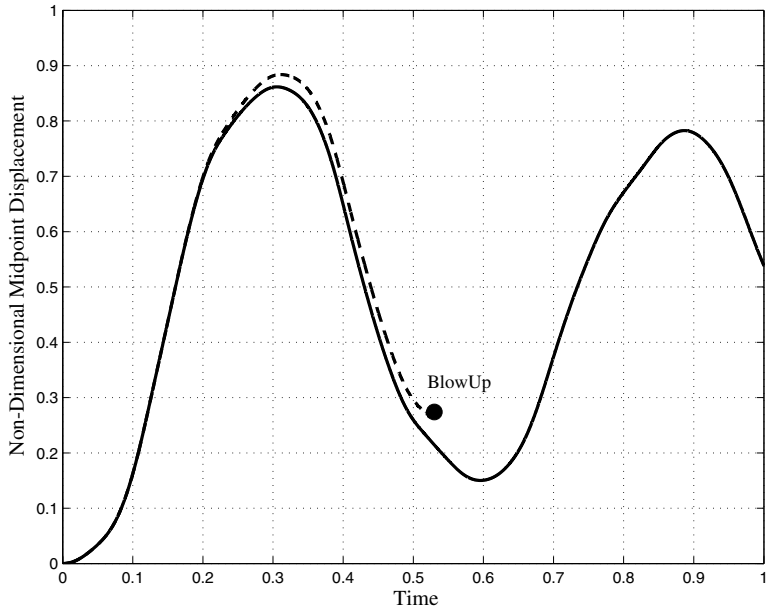

Fig. 8. The midpoint displacement $w(1,1,t)$ for the full von-Kármán system (Dashed line) and the system with the mixed derivative terms in 2,3 removed (Solid line). $N = 13$, $\Delta t = 10^{-6}$, $h = 0.1$, $c = 1.25$, $g = 29.60$, Fixed point conv. tolerance 10^{-10}. No filtering was used.

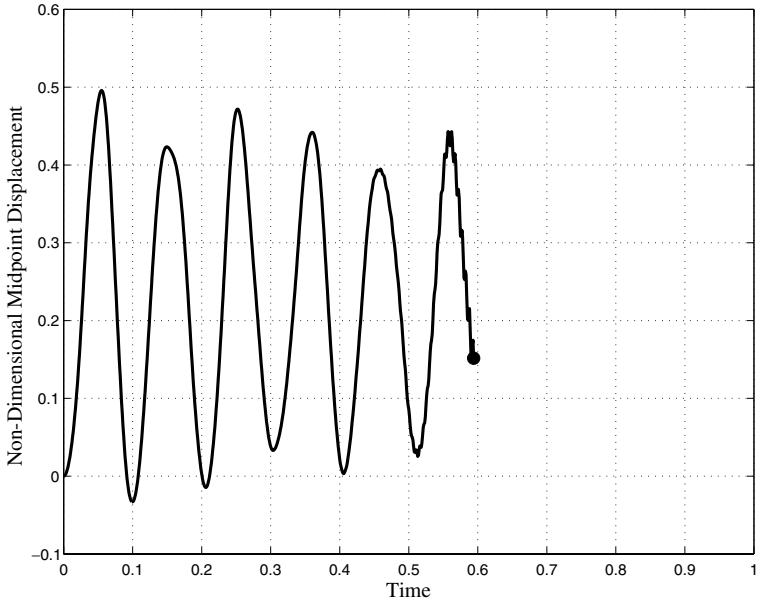

Fig. 9. The midpoint displacement $u(1,1,t)$ for the simplified system (Eqs. (28) and (29)). $N = 13$, $\Delta t = 10^{-5}$, $h = 0.1$, $c = 1.25$, $f_1 = f_2 = 1.0$, Fixed point conv. tolerance 10^{-10}. No filtering was used. The circle denotes the approximate time at which the solution becomes unstable.

In Section 4, we provide a detailed analysis which explains why these terms emit unstable solutions and present an alternative to the Chebyshev-collocation method for solving the full von-Kármán system which does not admit instabilities due to the cross-derivative terms.

4. Stability analysis

In our examination of Eqs. (2) and (3), we observed numerically that removal of the cross-derivative terms produced a numerically stable scheme. As demonstrated, the explosive growth witnessed was not a function of the non-linearity (which would commonly be blamed under such circumstances), nor was it a consequence of the time stepping algorithm chosen (again, a common component upon which instability is blamed), but due to the spatial discretization of the linear terms in Eqs. (2) and (3). In this section, we first show that the Chebyshev-collocation discretization of the spatial operators is consistent (the spatial numerical derivatives converge to the exact ones). Then we show through Kreiss analysis that the continuous linear problem is well-posed. We examine through eigenvalue analysis the discrete system obtained using a collocation spatial discretization, demonstrating that discretizing the cross-derivative terms using the Chebyshev-collocation method *for second-order time problems* yields an unstable solution regardless of the time stepping algorithm employed. Finally, we demonstrate through eigenanalysis that the Legendre-collocation method does not suffer from the is problem, and we further provide a proof that a Legendre-collocation scheme applied to the linear system given by Eqs. (28) and (29) is stable.

4.1. Consistency of the linear terms

Given the results in the previous section, one may hypothesize that the Chebyshev-collocation scheme applied to the spatial derivative terms in Eqs. (28) and (29) were inconsistent. To establish the validity of this hypothesis, we consider the following simple linear system:

$$\begin{aligned} &2u_{,11} + (1+\nu)v_{,12} + (1-\nu)u_{,22} = A_1, \\ &2v_{,22} + (1+\nu)u_{,12} + (1-\nu)v_{,11} = A_2, \end{aligned} \tag{30}$$

with $\nu = 0.3$. Let us assume that we are given u and v of the following form:

$$\begin{aligned} u &= \sin(\pi x_1)\sin(2\pi x_2), \\ v &= \sin(2\pi x_1)\sin(\pi x_2) \end{aligned} \tag{31}$$

from which we can derive the resulting functions A_1 and A_2. Given a spatial discretization of $N \times N$ Chebyshev–Gauss–Lobatto points, we evaluate the functions A_1 and A_2 at the grid points. We then use the Chebyshev collocation method to determine the approximate values of u and v at the grid points. Since we know the true solution for u and v analytically, we can determine the point-wise L_∞ error (maximum absolute difference evaluated at the grid points) between the true u and approximate u and between the true v and the approximate v. For the scheme to be consistent, we require that the error decrease *at least* in a first-order algebraic sense with increasing N. In Fig. 10, we plot the discrete L_∞ error as a function of N.

One observes the *exponential* convergence rate, manifested by the straight line in the log-linear graph. This clearly demonstrates the consistency of the numerical scheme being used and also demonstrates the expected superb converge property of the Chebyshev collocation.

Hence the Chebyshev-collocation scheme applied to the linear terms is consistent. This led us to question if the time-dependent linear system given by Eqs. (28) and (29) was even well-posed.

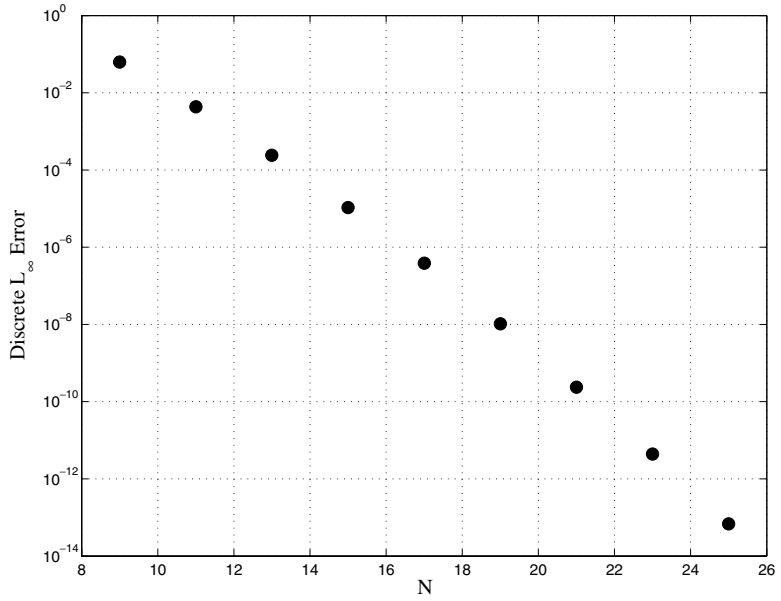

Fig. 10. The discrete L_∞ error in u as a function of N.

4.2. Stability analysis of the continuous linear system

In this section, we examine whether the time-dependent linear system given by Eqs. (28) and (29) solved as a periodic problem is well-posed. The analysis presented herein is not aimed to prove well-posedness of the problem *with* boundary conditions, but at gaining the insight into what might be the cause of the instability. The proof provided in Section 4.4 with respect to the numerical schemes of interest can easily be modified to show that the continuous system with boundary conditions is well-posed. Without loss of generality, we examine the following system:

$$u_{,tt} = 2u_{,11} + (1+v)v_{,12} + (1-v)u_{,22}, \tag{32}$$

$$v_{,tt} = (1-v)v_{,11} + (1+v)u_{,12} + 2v_{,22}, \tag{33}$$

where the linear dissipation term (the first time derivative term) has been removed. We examine through Kreiss analysis [18] whether the linear terms are well-posed for the periodic problem . Let us assume that we are interested in understanding Eqs. (32) and (33) with periodic boundary conditions on $[0,2\pi]\times[0,2\pi]$ with given initial condition $u_0(x_1,x_2) = u(x_1,x_2,t=0)$ and $v_0(x_1,x_2) = v(x_1,x_2,t=0)$.

Let us denote by $\mathbf{u}$ the vector $\mathbf{u}(x_1,x_2,t) = (u(x_1,x_2,t)\ v(x_1,x_2,t))^{\mathrm{T}}$. We can thus write the system (32) and (33) in the form:

$$\mathbf{u}_{,tt} = \begin{pmatrix} 2 & 0 \\ 0 & (1-v) \end{pmatrix}\mathbf{u}_{,11} + \begin{pmatrix} 0 & (1+v) \\ (1+v) & 0 \end{pmatrix}\mathbf{u}_{,12} + \begin{pmatrix} (1-v) & 0 \\ 0 & 2 \end{pmatrix}\mathbf{u}_{,22}. \tag{34}$$

Assuming a solution of the form $\mathbf{u}(x_1,x_2,t) = \mathrm{e}^{st}\mathrm{e}^{\mathrm{i}\alpha x_1}\mathrm{e}^{\mathrm{i}\beta x_2}\mathbf{c}$, with $\alpha,\beta\in\mathbb{R}$, $s\in\mathbb{C}$ and $\mathbf{c} = (c_1(x_1,x_2), c_2(x_1,x_2))^{\mathrm{T}}$, then substituting this expression into (34) yields the following:

$$s^2\mathbf{c} = -\alpha^2\begin{pmatrix} 2 & 0 \\ 0 & (1-\nu) \end{pmatrix}\mathbf{c} - \alpha\beta\begin{pmatrix} 0 & (1+\nu) \\ (1+\nu) & 0 \end{pmatrix}\mathbf{c} - \beta^2\begin{pmatrix} (1-\nu) & 0 \\ 0 & 2 \end{pmatrix}\mathbf{c}$$
$$= -\begin{pmatrix} 2\alpha^2 + (1-\nu)\beta^2 & \alpha\beta(1+\nu) \\ \alpha\beta(1+\nu) & \alpha^2(1-\nu) + 2\beta^2 \end{pmatrix}\mathbf{c} \stackrel{\text{def}}{=} -\mathbf{A}_c\mathbf{c}, \tag{35}$$

where $\mathbf{A}$ is a 2×2 real matrix.

Observe that Eq. (35) is nothing more than an eigenvalue problem of the matrix $\mathbf{A}_c$. To determine the well-posedness of the system, we must establish if the eigenvalues of $\mathbf{A}_c$ are positive; if they are positive, this implies that $-s^2$ is a positive number, i.e., s has to be a purely complex number and hence the solution to Eqs. (32) and (33) is not growing or decaying. To determine the sign of the two eigenvalues, we need only examine the first entry of the matrix $\mathbf{A}_c$ and the determinant of $\mathbf{A}_c$ [19]. Examining the first entry of $\mathbf{A}_c$, we see that $2\alpha^2 + (1-\nu)\beta^2 > 0$ because $0 \leqslant \nu \leqslant 0.5$. Furthermore,

$$\det(\mathbf{A}_\mathbf{c}) = (2\alpha^2 + (1-\nu)\beta^2)(\alpha^2(1-\nu) + 2\beta^2) - (1+\nu)^2\alpha^2\beta^2 = 2(1-\nu)(\alpha^2+\beta^2)^2 > 0. \tag{36}$$

We hence conclude that $\mathbf{A}_c$ is positive definite and hence both eigenvalues of positive. This implies that $-s^2 > 0$, and thus s is a pure imaginary number which yield oscillatory, non-growing solutions of the continuous system. The primary observation we deduced from this analysis was that the cross-derivative terms, when applied to a complex exponential ansatz, still yield terms which are purely negative real values. This observation sparked us to inquire as to the eigenstructure of the discrete system – specifically, did the eigenstructure of the discrete system have similar properties as those found in the analysis above? We examine the answer to this question in the next section.

4.3. Examination of the discrete system

Suppose that we discretize (32) and (33) with a Chebyshev- or Legendre-collocation method and enforce zero Dirichlet boundary conditions (as specified by the problem). We obtain the a set of algebraic equations which can be written in the form:

$$\frac{\mathrm{d}^2\tilde{\mathbf{u}}}{\mathrm{d}t^2} = \mathbf{A}\tilde{\mathbf{u}}, \tag{37}$$

where $\tilde{\mathbf{u}}$ is a vector of grid values for both u and v, and $\mathbf{A}$ denotes the discrete operator. At this stage, we are not specifying which collocation method we have chosen (Legendre or Chebyshev); although the matrix $\mathbf{A}$ will be different based upon this choice, the analysis below can be done for the arbitrary case.

Upon examination of the eigenvalues of $\mathbf{A}$ in the expression above when using the Chebyshev-collocation method, we observed the following. If the cross-derivative terms $u_{,12}$ and $v_{,12}$ are present in the equations, we obtain eigenvalues which have negative real parts but which have non-zero imaginary parts (as seen in Fig. 11 for differing values of N).

If the cross-derivatives $u_{,12}$ and $v_{,12}$ are omitted, then the eigen-values of the Chebyshev-collocation operator are all negative real (as seen in Fig. 12 for differing values of N).

Eigenvalues with negative real parts but non-zero imaginary parts yield unstable solutions. To prove this statement, we assume a solution of the form

$$\tilde{\mathbf{u}} = \mathrm{e}^{st}\tilde{\mathbf{c}},$$

where now $\tilde{\mathbf{c}} \in \mathbb{C}^n$ (n is the rank of $\mathbf{A}$) is an eigenvector of the matrix $\mathbf{A}$.

Substituting the assumed solution into Eq. (37) yields

$$s^2\tilde{\mathbf{c}} = \mathbf{A}\tilde{\mathbf{c}},$$

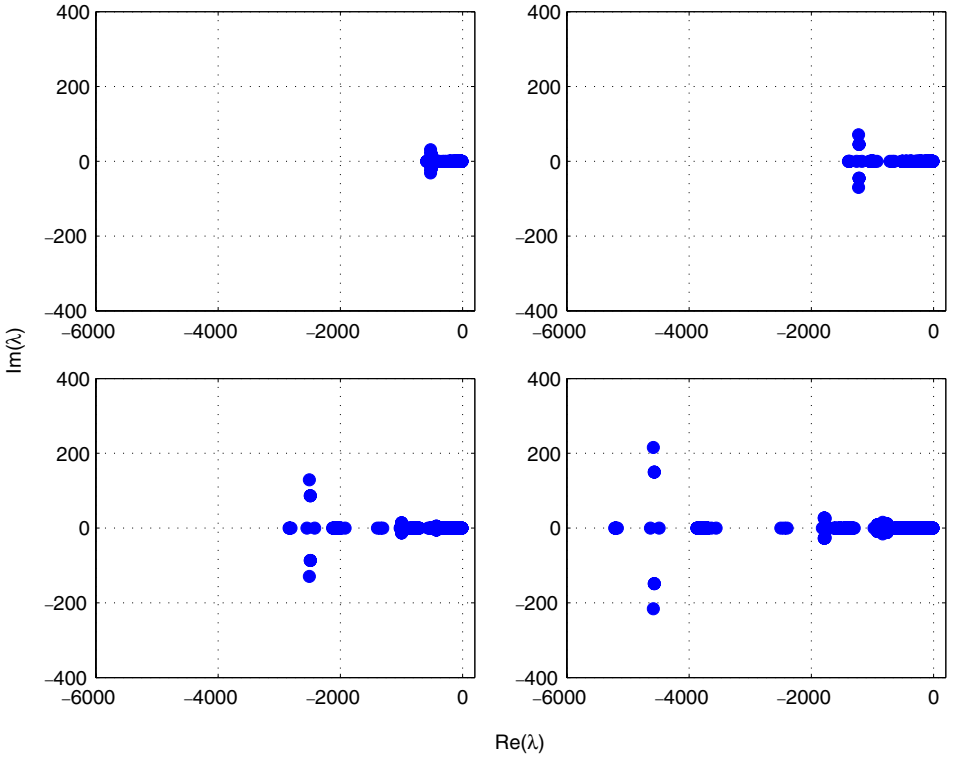

Fig. 11. Chebyshev-collocation: Eigenvalues for the discretized operator of (34) for $N = 9$ (upper left), $N = 11$ (upper right), $N = 13$ (lower left), $N = 15$ (lower right).

where, analogous to the work before, s^2 represents an eigenvalue of $\mathbf{A}$ (notice that here we use $\mathbf{A}$ instead of $-\mathbf{A}$ used in the continuous case because we do not have the negative sign due to the squaring of the imaginary parts of our assumed solution).

Let us assume that we denote an eigenvalue of $\mathbf{A}$ by $\xi = (\xi_r + i\xi_i) \in \mathbb{C}$ with real part $\xi_r \in \mathbb{R}$ and imaginary part $\xi_i \in \mathbb{R}$. We thus have that:

$$s^2 = \xi_r + i\xi_i.$$

Since s is a complex number, let us assume that it can be written in the form $s = s_r + is_i$, where $s_r, s_i \in \mathbb{R}$. Hence:

$$s^2 = (s_r + is_i)^2 = (s_r^2 - s_i^2) + 2is_r s_i = \xi_r + i\xi_i.$$

Seeking to solve this system, we observe that the following must be true:

$$s_r^2 - s_i^2 = \xi_r, \tag{38}$$

$$2s_r s_i = \xi_i. \tag{39}$$

We now investigate two possible cases of interest:

Case 1. Assume that $\xi_r < 0$ and $\xi_i = 0$

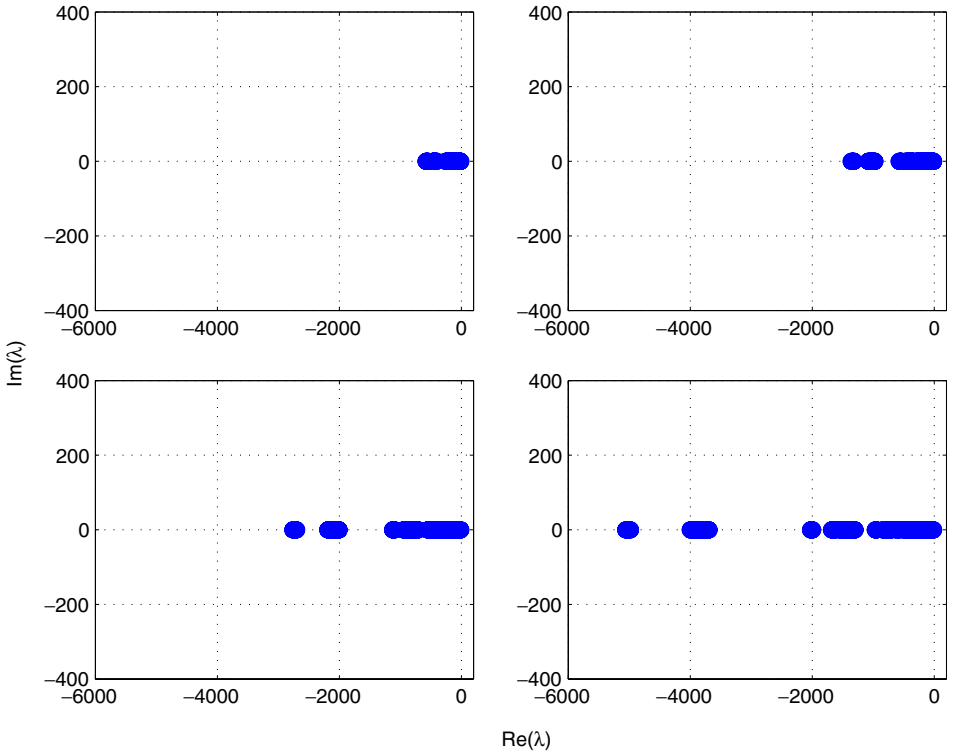

Fig. 12. Chebyshev-collocation: Chebyshev-collocation: Eigenvalues for the discretized operator of (34) without the mixed derivatives $u_{,12}$ and $v_{,12}$ for $N = 9$ (upper left), $N = 11$ (upper right), $N = 13$ (lower left), $N = 15$ (lower right).

If $\xi_i = 0$, either $s_r = 0$ or $s_i = 0$. Since we have assumed that $\xi_r < 0$ (which is the case of interest), the first equation implies that $s_r = 0$. As a consequence, we observe that we merely have oscillatory solutions ($s_i \neq 0$), which implies that our ODE solution has time oscillatory solutions of the form $e^{is_i t}\tilde{c}$. This scenario represents the case in which the cross-derivative terms were removed from the linear system.

Case 2. Assume that $\xi_r < 0$ and $\xi_i \neq 0$

If $\xi_i \neq 0$, then both $s_r \neq 0$ and $s_i \neq 0$ by the second equation. Since neither is zero, we can re-write the system to obtain the following:

$$s_r^4 - \xi_r s_r^2 - \tfrac{1}{4}\xi_i^2 = 0,$$

which yields admissible solutions of the form:

$$s_r = \pm\frac{1}{2}\sqrt{2\xi_r \pm 2\sqrt{\xi_r^2 + \xi_i^2}}.$$

This in turn allows both decaying and growing solutions. As a consequence, if the discretized operator has imaginary eigen-values, the scheme is unstable. This is precisely the scenario which arises when the Chebyshev-collocation method is used to solve the linear system given by Eqs. (32) and (33).

Through experimentation, we observed the following. If the Legendre-collocation method is used to form Eq. (37), then the eigen-values of the discretized operator are purely negative real. In Fig. 13, we

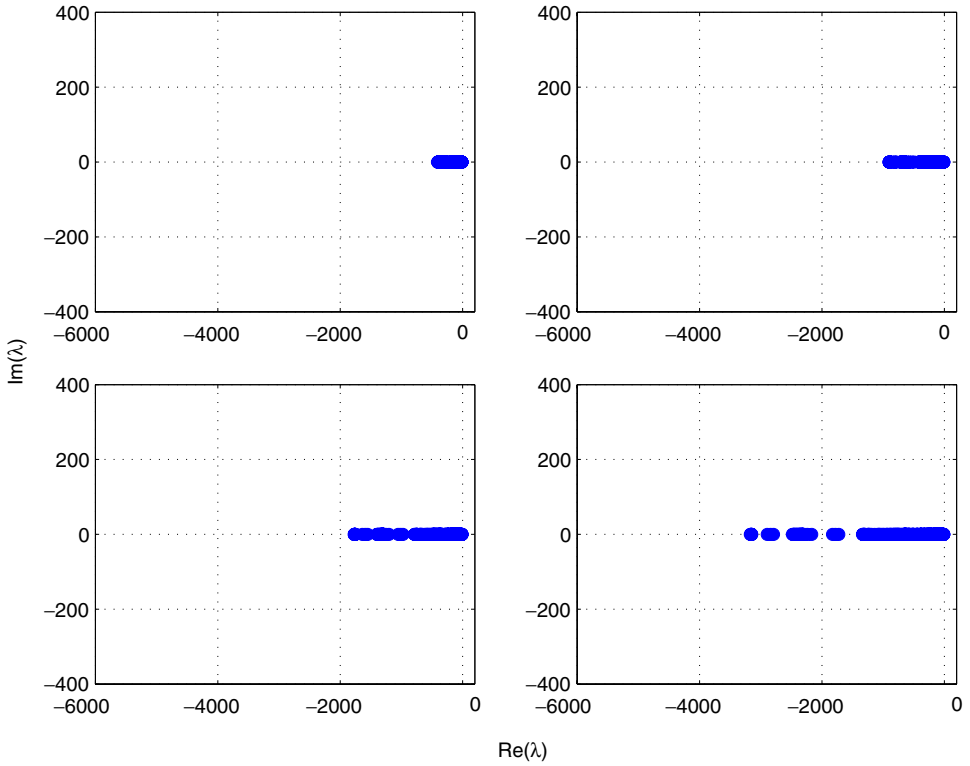

Fig. 13. Legendre-collocation: Eigenvalues for the discretized operator of (34) for $N = 9$ (upper left), $N = 11$ (upper right), $N = 13$ (lower left), $N = 15$ (lower right).

present them for $N = 9$, 11, 13, 15. This figure shows that in spite of the mixed derivatives, the discretized system equation (34) is stable when using the Legendre-collocation method.

To demonstrate empirically that the Legendre-collocation method is stable for the linear system, we solve our previously discussed linear test problem given by Eqs. (28) and (29) with the Legendre-collocation method. As before, we take $N = 13, \Delta t = 10^{-5}$, $c = 1.25$, $h = 0.1$, $f_1 = f_2 = 1.0$ and a Fixed point conv. tolerance 10^{-10}. In Fig. 14, we present both the stable Legendre-collocation result (solid line) and the previously discussed unstable Chebyshev-collocation result (dashed line).

This empirical test demonstrates that unlike the Chebyshev-collocation method, the Legendre-collocation method provides stable solutions. In the next section, we present a stability proof for the Legendre-collocation method applied to Eqs. (32) and (33).

4.4. Proof of stability for the Legendre-collocation method

We now prove that the linear system given by Eqs. (32) and (33) with homogeneous Dirichlet boundary conditions is stable when utilizing the Legendre-collocation method, and we, in the process, provide further insight into why the Chebyshev-collocation method is unstable for this problem.

Consider the system given in Eqs. (32) and (33) written in matrix form as given in Eq. (34):

$$\mathbf{u}_{,tt} = \mathbf{A}\mathbf{u}_{,11} + \mathbf{B}\mathbf{u}_{,12} + \mathbf{C}\mathbf{u}_{,22} \tag{40}$$

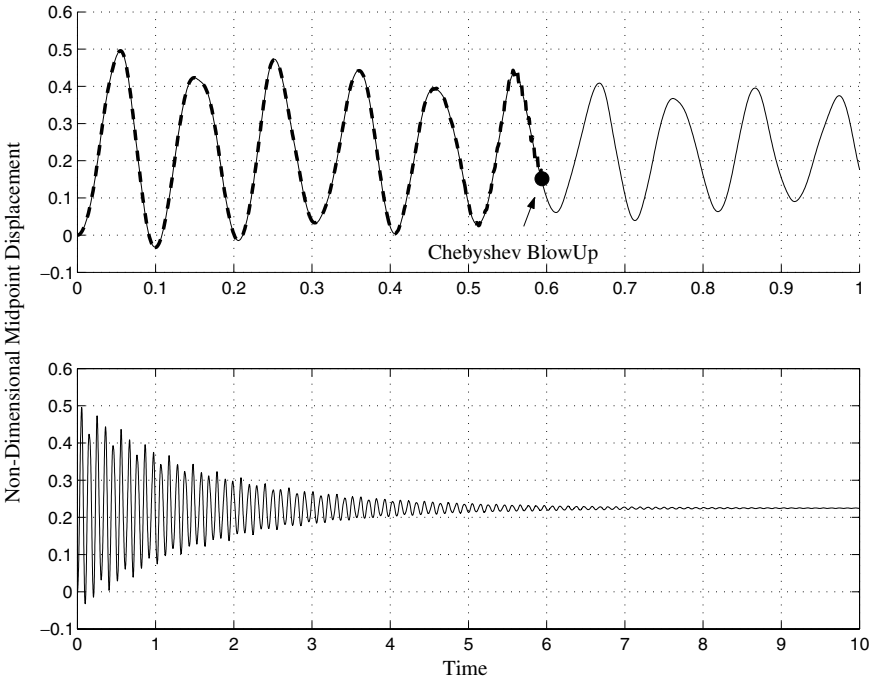

Fig. 14. Chebyshev-collocation and Legendre-collocation: Solution of Eqs. (28) and (29) with $N = 13, \Delta t = 10^{-5}, c = 1.25, h = 0.1$, $f_1 = f_2 = 1.0$ and Fixed point conv. tolerance 10^{-10}. No filtering was used.

satisfied, without loss of generality, on $[-1,1] \times [-1,1]$, with homogeneous boundary conditions $\mathbf{u}(x_1, x_2) = 0$ on the boundary, and where $\mathbf{A}$, $\mathbf{B}$, and $\mathbf{C}$ are symmetric matrices (as given in Eq. (34)) which have the property that for every vector $\mathbf{v}(x_1, x_2)$

$$\mathbf{v}_{,1}^{\mathrm{T}}\mathbf{A}\mathbf{v}_{,1} + \mathbf{v}_{,1}^{\mathrm{T}}\mathbf{B}\mathbf{v}_{,2} + \mathbf{v}_{,2}^{\mathrm{T}}\mathbf{C}\mathbf{v}_{,2} > 0.$$

The Legendre-collocation approximation to Eq. (40) involves seeking a polynomial vector $\tilde{\mathbf{u}}(x_1, x_2, t)$ of degree N such that

$$\frac{\partial^2 \tilde{\mathbf{u}}}{\partial t^2} = \mathbf{A}\tilde{\mathbf{u}}_{,11} + \mathbf{B}\tilde{\mathbf{u}}_{,12} + \mathbf{C}\tilde{\mathbf{u}}_{,22} \tag{41}$$

is satisfied at the Gauss–Lobatto–Legendre (GLL) points $(x_1)_j, (x_2)_k$, $j,k = 1, \ldots, N-1$, and the boundary conditions are imposed strongly, i.e., $\tilde{\mathbf{u}}((x_1)_0, (x_2)_k) = \tilde{\mathbf{u}}((x_1)_N, (x_2)_k) = \tilde{\mathbf{u}}((x_1)_k, (x_2)_0) = \tilde{\mathbf{u}}((x_1)_k, (x_2)_N) = 0$. Here, and throughout this section, we will assume that given the point value vector $\tilde{\mathbf{u}}$ one can form the interpolating polynomial as given in Eq. (5). Hence, we will use the notation $\tilde{\mathbf{u}}$ to designate the point values and hence also the interpolating polynomial that can be formed based upon those values.

We define for any polynomial (grid) value vectors $\tilde{\mathbf{f}}, \tilde{\mathbf{g}}$ the scalar product:

$$(\tilde{\mathbf{f}}, \tilde{\mathbf{g}})_h = \sum_{j=0}^{N} \sum_{k=0}^{N} \tilde{\mathbf{f}}^{\mathrm{T}}((x_1)_j, (x_2)_k)\tilde{\mathbf{g}}((x_1)_j, (x_2)_k)\omega_j\omega_k, \tag{42}$$

where ω_j are the weights given in the GLL quadrature formula [12]. The 'h' denotes that this is a discretized (quadrature) version of the continuous L_2 inner product.

We begin with the following lemma which will be used in the proof of stability to follow.

Lemma 1. *Let* $\tilde{\mathbf{f}}, \tilde{\mathbf{g}}$ *be polynomial vectors of order* N *that vanish at the boundary points, then*

$$(\tilde{\mathbf{f}}, \tilde{\mathbf{g}}_{,1})_h = -(\tilde{\mathbf{f}}_{,1}, \tilde{\mathbf{g}})_h. \tag{43}$$

Proof 1. Recall the definition given above, namely:

$$(\tilde{\mathbf{f}}, \tilde{\mathbf{g}}_{,1})_h = \sum_{j=0}^{N} \sum_{k=0}^{N} \tilde{\mathbf{f}}^{\mathrm{T}}((x_1)_j, (x_2)_k) \tilde{\mathbf{g}}_{,1}((x_1)_j, (x_2)_k) \omega_j \omega_k. \tag{44}$$

The degree of the polynomial $\tilde{\mathbf{f}}^{\mathrm{T}}((x_1)_j, (x_2)_k)\tilde{\mathbf{g}}_{,1}((x_1)_j, (x_2)_k)$ in x_1 is $2N-1$ (since $\tilde{\mathbf{f}}$ is of order N in the x_1-direction and $\tilde{\mathbf{g}}_{,1}$ is of order $N-1$ in the x_1-direction), and therefore the GLL formula using $N+1$ points/weights is exact. Thus we have that

$$(\tilde{\mathbf{f}}, \tilde{\mathbf{g}}_{,1})_h = \sum_{k=0}^{N} \int_{-1}^{1} \tilde{\mathbf{f}}^{\mathrm{T}}(x_1, (x_2)_k) \tilde{\mathbf{g}}_{,1}(x_1, (x_2)_k) \, \mathrm{d}x_1 \omega_k.$$

Since $\tilde{\mathbf{f}}^{\mathrm{T}}\tilde{\mathbf{g}}$ vanishes at the boundaries we can integrate by parts and use again the GLL formula to yield:

$$(\tilde{\mathbf{f}}, \tilde{\mathbf{g}}_{,1})_h = -\sum_{k=0}^{N} \int_{-1}^{1} \tilde{\mathbf{f}}_{,1}^{\mathrm{T}}(x_1, (x_2)_k) \tilde{\mathbf{g}}(x_1, (x_2)_k) \, \mathrm{d}x_1 \omega_k \tag{45}$$

$$= -\sum_{j=0}^{N} \sum_{k=0}^{N} \tilde{\mathbf{f}}_{,1}^{\mathrm{T}}((x_1)_j, (x_2)_k) \tilde{\mathbf{g}}((x_1)_j, (x_2)_k) \omega_j \omega_k \tag{46}$$

$$= -(\tilde{\mathbf{f}}_{,1}, \tilde{\mathbf{g}}). \quad \square \tag{47}$$

In the same way as above we get the following lemma:

Lemma 2.

$$(\tilde{\mathbf{f}}, \tilde{\mathbf{g}}_{,2})_h = -(\tilde{\mathbf{f}}_{,2}, \tilde{\mathbf{g}}).$$

Observe that Lemma 1 *and* Lemma 2 *represent the fact that integration by parts can be accomplished exactly under these assumptions when using GLL quadrature. We are now ready for the main theorem of stability of the Legendre-collocation applied to solving* Eq. (40)*:*

Theorem (Stability). *Let* $\tilde{\mathbf{u}}$ *be the Legendre-collocation approximation to* Eq. (40) *given by* Eq. (41), *then*

$$(\tilde{\mathbf{u}}_{,t}, \tilde{\mathbf{u}}_{,t})_h(t) + (\tilde{\mathbf{u}}_{,1}, \mathbf{A}\tilde{\mathbf{u}}_{,1})_h(t) + (\tilde{\mathbf{u}}_{,1}, \mathbf{B}\tilde{\mathbf{u}}_{,2})_h(t) + (\tilde{\mathbf{u}}_{,2}, \mathbf{C}\tilde{\mathbf{u}}_{,2})_h(t) \tag{48}$$

$$= (\tilde{\mathbf{u}}_{,t}, \tilde{\mathbf{u}}_{,t})_h(0) + (\tilde{\mathbf{u}}_{,1}, \mathbf{A}\tilde{\mathbf{u}}_{,1})_h(0) + (\tilde{\mathbf{u}}_{,1}, \mathbf{B}\tilde{\mathbf{u}}_{,2})_h(0) + (\tilde{\mathbf{u}}_{,2}, \mathbf{C}\tilde{\mathbf{u}}_{,2})_h(0) \tag{49}$$

Proof 2. We start by observing the since $\tilde{\mathbf{u}}$ vanishes at the boundaries at any time t, so does $\tilde{\mathbf{u}}_t$ at the boundaries. We therefore multiply Eq. (41) by $\tilde{\mathbf{u}}_t$ and sum up over $j = 0, \ldots, N$, $k = 0, \ldots, N$. We thus obtain:

$$(\tilde{\mathbf{u}}_{,t}, \tilde{\mathbf{u}}_{,tt})_h = (\tilde{\mathbf{u}}_{,t}, \mathbf{A}\tilde{\mathbf{u}}_{,11})_h + (\tilde{\mathbf{u}}_{,t}, \mathbf{B}\tilde{\mathbf{u}}_{,12})_h + (\tilde{\mathbf{u}}_{,t}, \mathbf{C}\tilde{\mathbf{u}}_{,22})_h.$$

We use now Lemma 1 to obtain the following:

$$(\tilde{\mathbf{u}}_{,t}, \mathbf{A}\tilde{\mathbf{u}}_{,11})_h = -(\tilde{\mathbf{u}}_{,tx}, \mathbf{A}\tilde{\mathbf{u}}_{,1})_h = -\frac{1}{2}\frac{\mathrm{d}}{\mathrm{d}t}(\tilde{\mathbf{u}}_{,1}, \mathbf{A}\tilde{\mathbf{u}}_{,1})_h.$$

If we now use Lemmas 1 and 2 to re-write the other terms, we arrive at:

$$\frac{\mathrm{d}}{\mathrm{d}t}(\tilde{\mathbf{u}}_{,t}, \tilde{\mathbf{u}}_{,t})_h(t) + (\tilde{\mathbf{u}}_{,1}, \mathbf{A}\tilde{\mathbf{u}}_{,1})_h(t) + (\tilde{\mathbf{u}}_{,1}, \mathbf{B}\tilde{\mathbf{u}}_{,2})_h(t) + (\tilde{\mathbf{u}}_{,2}, \mathbf{C}\tilde{\mathbf{u}}_{,2})_h(t) = 0$$

hence proving the theorem, and proving that the energy of the system should be conserved for all time.

To understand why the Legendre-collocation method is stable (as defined above) and the Chebyshev-collocation method is not, consider the following simple model equation:

$$V_{,tt} = V_{,11} + \beta V_{,1},$$

on $[-1,1] \times [-1,1]$ with homogeneous boundary conditions and with β a real constant value.

The Legendre-collocation approximation $\tilde{\mathbf{v}}$ of the equation above satisfies

$$\tilde{\mathbf{v}}_{,tt} = \tilde{\mathbf{v}}_{,11} + \beta\tilde{\mathbf{v}}_{,1}$$

at the (internal) GLL grid points $x_1 = (x_1)_j,\ 1 \leqslant j \leqslant N-1$ (the boundary points are irrelevant due to the homogeneous boundary conditions).

Applying the methodology previously used, one immediately gets that:

$$(\tilde{\mathbf{v}}_{,t}, \tilde{\mathbf{v}}_{,t}) + (\tilde{\mathbf{v}}_{,1}, \tilde{\mathbf{v}}_{,1}) = 0.$$

This implies that the operator

$$\frac{\mathrm{d}^2}{\mathrm{d}x_1^2} + \beta\frac{\mathrm{d}}{\mathrm{d}x_1}$$

operating on the space of polynomials has real negative eigenvalues, explaining the stability of the method.

However in the Chebyshev scalar product, the above operator has complex eigenvalues (with negative real parts). This implies stability for the parabolic equation (first-order in time) but instability if the left-hand-side is $\tilde{\mathbf{v}}_{,tt}$ (second-order in time).

Hence, in this section we have provided a mathematical proof as to the stability of the Legendre-collocation method applied to the system given in Eqs. (32) and (33), and have provided a brief explanation (based upon the methodology provided in the proof) as to why the Chebyshev-collocation method is not appropriate for this system.

5. Legendre-collocation: Full von-Kármán system

We now return to examining the full von-Kármán system, this time applying the Legendre-collocation method for the spatial discretization. We then examine the Chebyshev-collocation system with in-plane filtering (as presented in [1]), the Chebyshev-collocation simplified von-Kármán system (as also presented in [1]) and the new Legendre-collocation method.

5.1. Solution of the full system for the Legendre-collocation method

Consider again the constant load $g = 29.6$ applied on the plate having a thickness $h = 0.1$ and $c = 1.25$. We use herein the Legendre-collocation method with a 13×13 collocation grid and $\Delta t = 10^{-6}$

and report the midpoint deflection $w(1,1,t)$ in Fig. 15, and $u(0.29,0.29,t)$ and $v(0.29,0.29,t)$ in Fig. 16.

The solution is now stable for a much larger time, until $t \approx 9$. From our previous analysis, we know that the Legendre-collocation method is stable for the linear problem. We postulate that the scheme suffers from instability due to the collocation treatment of the non-linear terms (a well-known problem of collocation methods [12]). A stable solution is observed for relatively long times until instabilities finally occur. To alleviate the problem, we apply a filter to the non-linear terms in the in-plane (u and v) equations as advocated in [20] for hyperbolic problems of this form.

We use the exponential filtering (15) with a $p = 4$ filter on the non-linear terms in the in-plane equations (as in Section 2.3) and plot in Fig. 17 the midpoint deflection $w(1,1,t)$ for same discretization parameters. Fig. 17 demonstrates the filtering influence in stabilizing the numerical solution (damping the high frequencies) without imposing large numerical errors. To better visualize this fact we plot in Fig. 18 the relative difference between the filtered and non-filtered solutions:

$$\text{Relative difference} = \left| \frac{w_{\text{No filtering}} - w_{\text{Filtered}}}{w_{\text{Filtered}}} \right|.$$

A small difference of less than 1% is noticed for all times until the instability.

The relative errors (comparing the filtered and unfiltered numerical solutions), in the displacement fields u and v are of the same order of magnitude as the error in w and have not been shown herein.

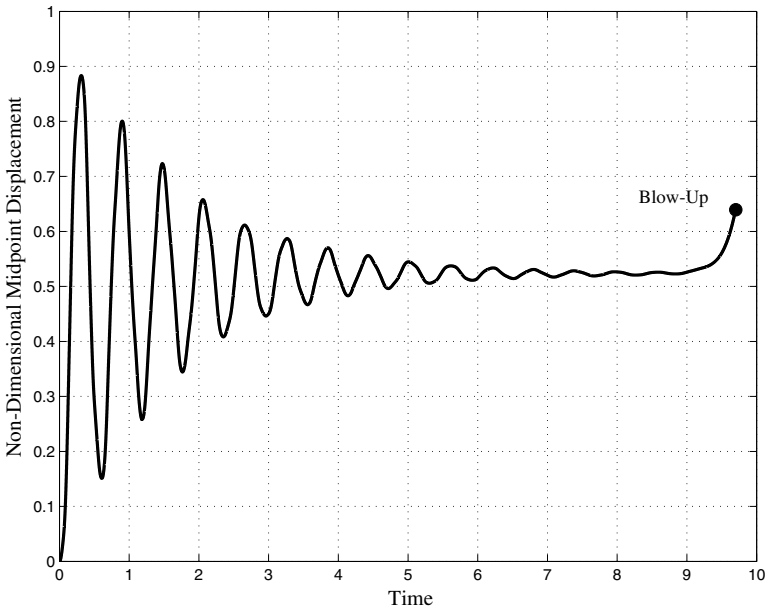

Fig. 15. Legendre-collocation: Midpoint displacement $w(1,1,t)$. $N = 13$, $\Delta t = 10^{-6}$, $h = 0.1$, $c = 1.25$, $g = 29.60$, Fixed point conv. tolerance 10^{-10}. No filtering was used.

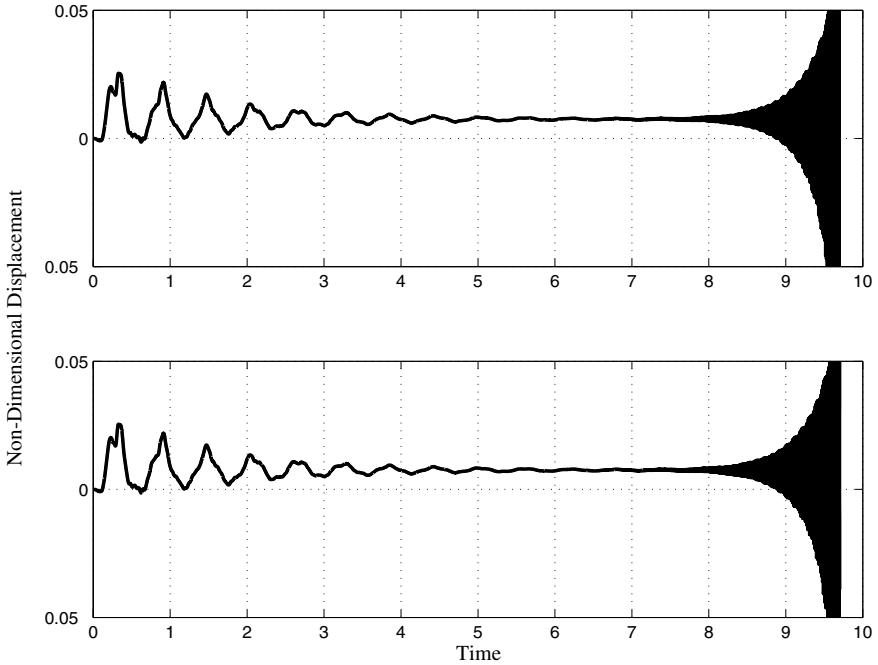

Fig. 16. Legendre-collocation: In-plane displacements at an offset point $u(0.29, 0.29, t)$ (top) and $v(0.29, 0.29, t)$ (bottom). $N = 13$, $\Delta t = 10^{-6}$, $h = 0.1$, $c = 1.25$, $g = 29.60$, Fixed point conv. tolerance 10^{-10}. No filtering was used.

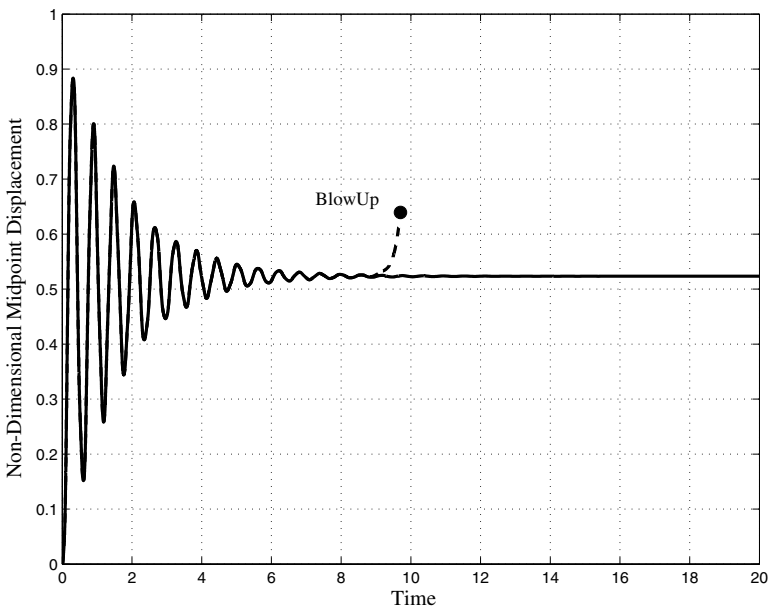

Fig. 17. Legendre-collocation: Midpoint displacement $w(1, 1, t)$ with Exponential filtering $p = 4$ (solid line), and without filtering (dashed line). $N = 13$, $\Delta t = 10^{-6}$, $h = 0.1$, $c = 1.25$, $g = 29.60$, Fixed point conv. tolerance 10^{-10}.

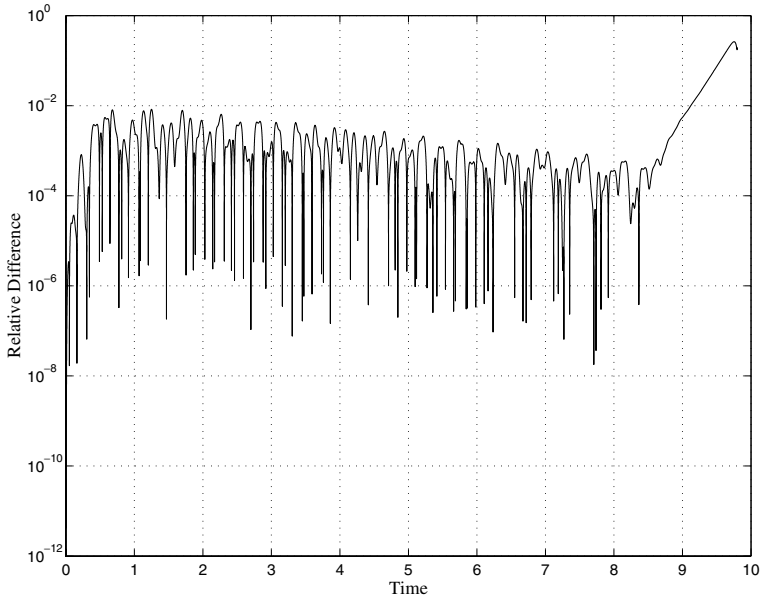

Fig. 18. Legendre-collocation: Relative difference in midpoint displacement $w(1,1,t)$ with and without filtering of the in-plane non-linear terms. $N = 13$, $\Delta t = 10^{-6}$, $h = 0.1$, $c = 1.25$, $g = 29.60$, Fixed point conv. tolerance 10^{-10}. Exponential filtering $p = 4$ was used.

5.2. Chebyshev with filtering of in-plane solutions, Legendre with exponential filtering of in-plane non-linear terms, Chebyshev and Nath and Kumar for simplified system

To further examine the schemes presented in this paper, we compare the Chebyshev-collocation method with in-plane filtering (as presented in [1]), the Chebyshev-collocation simplified von-Kármán system [2] (also presented in [1]), the Legendre-collocation with exponential filtering of the non-linear terms (as discussed above), and the published results of Nath and Kumar [6] (in [6] an error has been found in the von-Kármán system of equations as explained in [1]).

Taking $N = 13$, $\Delta t = 10^{-7}$, $h = 0.001$, $c = 1.25$, $g = 29.14$, Fixed point conv. tolerance 10^{-10}, we plot in Fig. 19 the aforementioned results (which all lie on the same solid black line) against the results of Nath and Kumar (denoted by the blue line with circles).

To help distinguish between the different results above, we plot in Fig. 20 the relative difference between the Chebyshev-collocation with in-plane filtering and the Chebyshev-collocation simplified system (dashed), and between the Legendre-collocation with exponential filtering ($p = 4$) of the in-plane non-linear terms and the Chebyshev-collocation simplified system (solid). Comparison between a Chebyshev-collocation simplified von-Kármán scheme and a Legendre-collocation simplified von-Kármán scheme under the same conditions yielded relative differences on the order of 10^{-3}.

In Fig. 21, we present a plot of the u displacement at an offset point $(x_1, x_2) = (0.29, 0.29)$ with respect to time for Chebyshev-collocation with in-plane filtering (dash-dot), Chebyshev-collocation simplified von-Kármán (solid), and Legendre-collocation with exponential filtering ($p = 4$) of the in-plane non-linear terms (dashed). As can be observed, all three methods are in very good agreement.

[2] Note that the simplified von-Kármán system presented in [1] does not suffer from numerical stability problems, and thus does not require any filtering.

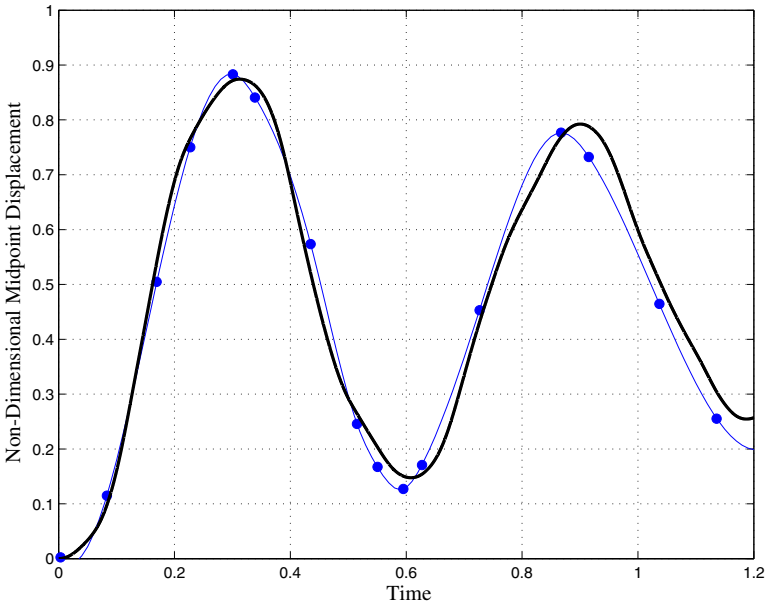

Fig. 19. Comparison: Midpoint displacement $w(1,1,t)$ for Chebyshev-collocation with in-plane filtering, Legendre-collocation with exponential filtering ($p = 4$) of the non-linear terms, Chebyshev-collocation of the simplified von-Kármán system (all lying on the solid black line) compared to the results of Nath & Kumar [6] (solid blue line with circles). $N = 13$, $\Delta t = 10^{-7}$, $h = 0.001$, $c = 1.25$, $g = 29.14$, Fixed point conv. tolerance 10^{-10}.

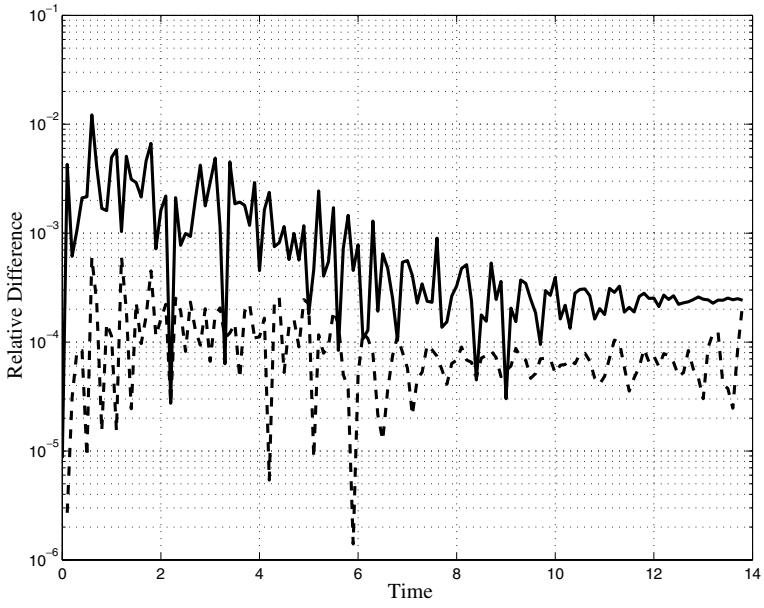

Fig. 20. Comparison: Relative difference in the midpoint displacement $w(1,1,t)$ between the Legendre-collocation with exponential filtering ($p = 4$) of the in-plane non-linear terms and the Chebyshev-collocation simplified von-Kármán system (solid) and between the Chebyshev-collocation with filtering of the in-plane solutions and the Chebyshev-collocation simplified von-Kármán system (dashed). $N = 13$, $\Delta t = 10^{-7}$, $h = 0.001$, $c = 1.25$, $g = 29.14$, Fixed point conv. tolerance 10^{-10}.

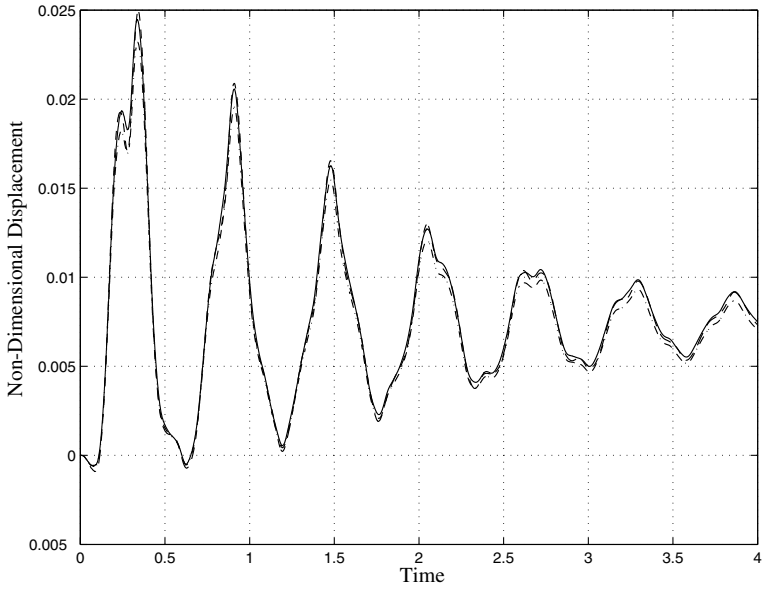

Fig. 21. Comparison: $u(0.29, 0, 29, t)$ displacement for Chebyshev-collocation with in-plane filtering (dash-dot), Legendre-collocation with exponential filtering ($p = 4$) of the non-linear terms (dashed), and Chebyshev-collocation of the simplified von-Kármán system (solid). $N = 13$, $\Delta t = 10^{-7}$, $h = 0.001$, $c = 1.25$, $g = 29.14$, Fixed point conv. tolerance 10^{-10}.

6. Summary and conclusions

The von-Kármán non-linear, dynamic, partial differential system over rectangular domains was numerically solved using both the Chebyshev-collocation and Legendre-collocation methods for the spatial discretization and the implicit Newmark-β combined with a non-linear fixed point algorithm for the temporal discretization. We have highlighted the difficulties inherent in its numerical treatment, especially using the Chebyshev-collocation scheme considered in [1]. We showed that IC/BC incompatibilities are not the culprits of the instability sighted in [1], and demonstrated empirically that the source of the instability was the numerical treatment of the *linear* cross-derivative terms found in the in-plane equations. We proved that although the continuous linear system is well-posed, the Chebyshev-collocation solution of problems involving cross-derivatives and second-order time derivatives is unstable.

By employing the Legendre-collocation method, we proved that the scheme for the linear system has the necessary characteristics to remain stable. Nevertheless, the collocation treatment of the non-linear terms still caused the solution to be unstable at long time, so using an exponential filtering only on the *non-linear* terms (to compensate for the inherent aliasing error due to our collocation treatment of these) we stabilized the scheme. We concluded by comparing the results of filtered Chebyshev-collocation solution, non-linear terms filtered Legendre-collocation solution, and a simplified von-Kármán (solution omitting the inertial terms in the in-plane equations). This comparison showed that the simplified von-Kármán system and the filtered Legendre-collocation solution provide results of excellent agreement.

Preliminary numerical studies considering the complete von-Kármán set of equations with the additional term $-(h^2/12)\Delta w_{,tt}$ in (1) shows that:

- The term's effect decreases as the thickness decreases (which is expect).
- The Chebyshev-collocation method and the Legendre-collocation method perform similarly with or without the rotational inertia term.

This work has been motivated by a broader research project in which a fluid–structure interaction of a plate embedded in a flow field has to be investigated (see, e.g. [8]). Towards this end, we have demonstrated that using the simplified von-Kármán system, thus enabling a large time step to be used, is justified and introduces minor modeling errors.

Acknowledgements

The authors thank Prof. George Em Karniadakis of the Division of Applied Mathematics at Brown University, Providence, RI, for helpful discussions, remarks and support. The first author gratefully acknowledges the support of this work by the Air Force Office of Scientific Research (Computational Mathematics Program) under Grant No. F49620-01-1-0035. The second author gratefully acknowledges the computational support and resources provided by the Scientific Computing and Imaging Institute at the University of Utah.

References

[1] R.M. Kirby, Z. Yosibash, Solution of von-Kármán dynamic non-linear plate equations using a pseudo-spectral method, Comput. Meth. Appl. Mech. Engrg. 193 (6–8) (2004) 575–599.
[2] I. Lasiecka, Uniform stabilizability of a full von Karman system with nonlinear boundary feedback, SIAM J. Control Optim. 36 (4) (1998) 1376–1422.
[3] H. Koch, I. Lasiecka, Hadamard well-posedness of weak solutions in nonlinear dynamic elasticity-full von Karman systems, Progr. Nonlinear Differenatial Equations 50 (2002) 197–216.
[4] Chuen-Yuan Chia, Nonlinear Analysis of Plates, McGraw-Hill, 1980.
[5] W. Han, M. Petyt, Geometrically nonlinear vibration analysis of thin, rectangular plates using the hierarchical finite element method – I: The fundamental mode of isotropic plates, Comp. Struct. 63 (1997) 295–308.
[6] Y. Nath, S. Kumar, Chebyshev series solution to non-linear boundary value problems in rectangular domain, Comput. Meth. Appl. Mech. Engrg. 125 (1995) 41–52.
[7] R.E. Gordnier, R. Fithen, Coupling of a nonlinear finite element structural method with Navier–Stokes solver. AIAA2001-2853, in: 31st Fluid Dynamics Conference, June 2001.
[8] R.E. Gordnier, M.R. Visbal, Development of a three-dimensional viscous aeroelastic solver for nonlinear panel flutter, J. Fluids Struct. 16 (2002) 497–527.
[9] John E. Lagnese, Boundary Stabilization of Thin Plates, SIAM (1989).
[10] J.P. Boyd, N. Flyer, Compatibility conditions for time-dependent partial differential equations and the rate of convergence of Chebyshev and Fourier spectral methods, Comput. Meth. Appl. Mech. Engrg. 175 (1999) 281–309.
[11] Philippe G. Ciarlet, Plates and Junctions in Elastic Multi-structures. An Asymptotic Analysis. RMA 14, Springer, Masson, 1990.
[12] C. Canuto, M.Y. Hussaini, A. Quarteroni, T.A. Zang, Spectral Methods in Fluid Mechanics, Springer, New York, 1987.
[13] Lloyd N. Trefethen, Spectral Methods in Matlab, SIAM (2000).
[14] J.L. Humar, Dynamics of Structures, A.A. Balkema Publishers, 2002.
[15] B.A. Szabó, I. Babuška, Finite Element Analysis, Wiley, New York, 1991.
[16] George Em Karniadakis, Spencer J. Sherwin, Spectral/*hp* Element Methods for CFD, Oxford University Press, NY, USA, 1999.
[17] R. Burden, J.D. Faires, Numerical Analysis, PWS Publishing Company, 1993.
[18] H.O. Kreiss, J. Lorenz, Initial-boundary Value Problems and the Navier–Stokes Equations, Academic Press, 1989.
[19] G. Strang, Linear Algebra and Its Applications, Harcourt Brace Jovanovich College Publishers, 1998.
[20] D. Gottlieb, J.S. Hesthaven, Spectral methods for hyperbolic problems, J. Comput. Appl. Math. 128 (1-2) (2001) 83–131.